Renal expression of FGF23 and peripheral resistance to elevated FGF23 in rodent models of polycystic kidney disease

Spichtig, Daniela ; Zhang, Hongbo ; Mohebbi, Nilufar ; Pavik, Ivana ; Petzold, Katja ; Stange, Gerti ; Saleh, Lanja ; Edenhofer, Ilka ; Segerer, Stephan ; Biber, Jürg ; Jaeger, Philippe ; Serra, Andreas L ; Wagner, Carsten A

Abstract: Fibroblast growth factor 23 (FGF23) regulates phosphate homeostasis and is linked to cardiovascular disease and all-cause mortality in chronic kidney disease. FGF23 rises in patients with CKD stages 2-3, but in patients with autosomal dominant polycystic kidney disease, the increase of FGF23 precedes the first measurable decline in renal function. The mechanisms governing FGF23 production and effects in kidney disease are largely unknown. Here we studied the relation between FGF23 and mineral homeostasis in two animal models of PKD. Plasma FGF23 levels were increased 10-fold in 4-week-old cy/+ Han:SPRD rats, whereas plasma urea and creatinine concentrations were similar to controls. Plasma calcium and phosphate levels as well as TmP/GFR were similar in PKD and control rats at all time points examined. Expression and activity of renal phosphate transporters, the vitamin D3-metabolizing enzymes, and the FGF23 co-ligand Klotho in the kidney were similar in PKD and control rats through 8 weeks of age, indicating resistance to FGF23, although phosphorylation of the FGF receptor substrate 2 protein was enhanced. In the kidneys of rats with PKD, FGF23 mRNA was highly expressed and FGF23 protein was detected in cells lining renal cysts. FGF23 expression in bone and spleen was similar in control rats and rats with PKD. Similarly, in an inducible Pkd1 knockout mouse model, plasma FGF23 levels were elevated, FGF23 was expressed in kidneys, but renal phosphate excretion was normal. Thus, the polycystic kidney produces FGF23 but is resistant to its action.Kidney International advance online publication, 8 January 2014; doi:10.1038/ki.2013.526.

DOI: https://doi.org/10.1038/ki.2013.526

Renal Expression of FGF23 and Peripheral Resistance to elevated FGF23 in Rodent Models of Polycystic Kidney Disease

Daniela Spichtig[1*], Hongbo Zhang[1*], Nilufar Mohebbi[1,2], Ivana Pavik[1], Katja Petzold[1], Gerti Stange[1], Lanja Saleh[3], Ilka Edenhofer[1], Stephan Segerer[1,2], Jürg Biber[1], Philippe Jaeger[4], Andreas L. Serra[1,2#], and Carsten A. Wagner[1#]

[1]Institute of Physiology and Zurich Center for Integrative Human Physiology (ZIHP), University of Zurich, Zurich Switzerland,

[2]Division of Nephrology, University Hospital Zurich, Switzerland,

[3]Department of Clinical Chemistry, University Hospital Zurich, Switzerland

[4]Center for Nephrology, Royal Free Hospital, University College London, UK

*D. Spichtig and H. Zhang contributed equally to this study and share first authorship

#A. L. Serra and C. A. Wagner contributed equally to this study and share last authorship

Please send correspondence to:

Carsten A. Wagner
Institute of Physiology
University of Zurich
Winterthurerstrasse 190
CH-8057 Zurich
Switzerland
Phone: +41-44-63 55023
Fax : +41-44-63 56814
Email: Wagnerca@access.uzh.ch

ABSTRACT

Fibroblast growth factor 23 (FGF23) regulates phosphate homeostasis and is linked to cardiovascular disease and all-cause mortality in chronic kidney disease. FGF23 rises in patients with CKD stages 2-3 whereas in patients with autosomal dominant polycystic kidney disease (ADPKD), the increase of FGF23 precedes the first measurable decline in renal function. The mechanisms governing FGF23 production and effects in kidney disease are largely unknown. We examined the correlation between FGF23 and its effects on mineral homeostasis in two PKD animal models. Plasma FGF23 levels were 10-fold increased in 4 weeks old cy/+ Han:SPRD rats, whereas plasma urea and creatinine concentrations were similar to controls. Plasma calcium and phosphate levels as well as TmP/GFR were similar in PKD and control rats at all time points. Expression and activity of renal phosphate transporters, the vitamin D_3 metabolizing enzymes, and the FGF23 co-ligand Klotho in the kidney were similar in PKD and control rats at 2, 4 and 8 weeks, indicating resistance to FGF23. However, phosphorylation of the FRS2a protein was enhanced. In PKD kidneys FGF23 mRNA was highly expressed and FGF23 protein was detected in cells lining renal cysts. FGF23 expression in bone and spleen was similar in PKD and healthy animals. Similarly, in an inducible Pkd1 knockout mouse model plasma FGF23 levels were elevated, FGF23 was expressed in kidneys whereas renal phosphate excretion was normal. Thus, the polycystic kidney produces FGF23 but is resistant to it.

INTRODUCTION

Systemic phosphate homeostasis is regulated by a variety of factors including dietary intake, intestinal absorption, skeletal turnover, renal excretion, and systemic acid-base status as well as by many hormones. Among them parathyroid hormone (PTH), vitamin D_3, and fibroblast growth factor 23 (FGF23) act in concert at various levels of systemic phosphate homeostasis.[1-10]

FGF23 is a recently discovered member of the fibroblast growth factor family and is mainly expressed in bone and to a lesser extent in spleen, and brain but not in kidney.[11, 12] The kidney is the major target regulating phosphate reabsorption as well as vitamin D_3 metabolism.[13, 14] FGF23 acts on the distal convoluted tubule which may lead to the triggering of a cascade that reduces proximal tubular phosphate re-absorption.[15, 16] Alternatively in the proximal tubule FGF23 activates ERK1/2 and SGK1 phosphorylation (SGK1).[17] Phospho-SGK1 enables the phosphorylation of the sodium hydrogen exchanger regulatory factor (NHERF1) thereby allowing the internalization of the sodium phosphate cotransporter NaPi-IIa from the brush border membrane.[17] Consequently the reabsorption of phosphate from the glomerular fil-trate will decrease.[15-17] Furthermore, FGF23 reduces the plasma concentration of 1,25$(OH)_2$ vitamin D_3 through downregulation of Cyp27b1 (1α-hydroxylase) in the proximal tubule, the responsible enzyme for the 1α-hydroxylation of 25(OH) vitamin D_3, and the upregulation of Cyp24a1 (24-OHase), the responsible enzyme for the degradation of active 1,25$(OH)_2$ vitamin D_3.[13, 14]

The severe disturbance of phosphate homeostasis accounts for morbidity and mortality in patients with end-stage renal disease.[18] FGF23 is elevated in patients with CKD stages 2 and 3 whereas PTH increases significantly later.[19-22] In haemodi-alysis patients FGF23 contributes to the excessive morbidity and mortality independ-

ently of serum phosphate and PTH levels.[18] Moreover, CKD patients suffer from low vitamin D_3 which may be caused at least in part by high FGF23 levels.[20, 22, 23] Similarly, rats with progressive kidney disease showed elevated FGF23 levels.[24] In these animals, a neutralizing FGF23 antibody led to hyperphosphatemia and normalized $1,25(OH)_2$ vitamin D_3 levels.[24]

ADPKD is a slowly progressive disease that is manifested by the replacement of functional renal tissue with growing cysts.[25] The responsible mutations lie in the PKD1 and PKD2 genes, encoding the two transmembrane proteins polycystin-1 (PC1) and polycystin-2 (PC2), respectively.[26-30] ADPKD patients have 4-fold increased FGF23 levels even before renal function declines.[31] Among these patients, only those with normal soluble α-Klotho, showed a mild decrease in plasma phosphate values.[31, 32]

The Han:SPRD rat is a well-established PKD animal model with a mutation in the Pkdr1 gene that encodes the SamCystein protein.[33, 34] The slow progression of cystic kidney disease with a significant increase of creatinine and urea serum concentrations after 8 weeks is typical for heterozygous male animals (cy/+).[35] Cysts in the cy/+ animals originate mainly from the proximal tubule similar to mice with a deletion in the Pkd1 gene.[35, 36] The PKD model has been widely used for examining mechanisms and therapies for ADPKD.[37-40]

We investigated the regulation of renal phosphate handling, FGF23 expression, and production in two PKD animal models. We found that the polycystic kidney produces FGF23 but is resistant to it.

RESULTS

Plasma concentrations of FGF23 and PTH

FGF23 plasma concentrations were increased in cy/+ Han:SPRD rats compared with wild type (+/+) animals at all time points studied (Figure 1a). At week 2, the difference in FGF23 concentration between cy/+ (55 ± 27 pg/ml) and +/+ animals (35 ± 11 pg/ml) was 20 pg/ml (95 % CI 0.5 – 39pg/ml). FGF23 plasma levels further increased in cy/+ animals to 549 pg/ml after 4 weeks (mean difference 497 pg/ml, 95 % CI 444 – 549 pg/ml). FGF23 concentration in cy/+ animals remained approximately 10-fold higher at 6 and 8 weeks compared with controls. PTH plasma concentrations were similar in cy/+ and +/+ animals at 2 weeks (Figure 1b) whereas after 4 weeks, PTH levels of cy/+ animals were 2-fold elevated (141 ± 16 pg/ml) compared with +/+ animals (63 ± 6 pg/ml) (mean difference 78 pg/ml, 95 % CI 64 - 92pg/ml). PTH concentration in cy/+ animals remained 2-fold higher at 6 and 8 weeks.

The renal function parameters plasma creatinine and urea were similar for cy/+ and +/+ animals from birth to week 4, thereafter the values were higher in cy/+ compared with +/+ animals (Figures 1c and 1d). The estimated change of plasma creatinine per week in cy/+ animals was 2 µmol/l (95 % CI 1 - 3 µmol/l) and 0.8 µmol/l (95 % CI 0.7 – 1 µmol/l) in +/+ animals. For urea, the estimated change per week was 0.6 mmol/l (95 % CI 0.4 – 0.9 mmol/l) in cy/+ animals and 0.1 mmol/l (95 % CI 0.1 – 0.2 mmol/l) in +/+ animals. At week 4, we measured plasma phosphate and calcium as well as TmP/GFR and creatinine clearance of cy/+ and control Han:SPRD rats after an overnight fast (Supplementary Figure 1). All parameters were similar in both groups.

FGF23 expression in cystic kidneys

In order to identify the source(s) of elevated FGF23 in cy/+ Han:SPRD rats, we extracted mRNA from bone, kidney, spleen, heart, and liver and assessed FGF23 mRNA expression by semi-quantitative real-time PCR. In bone, FGF23 expression increased over time in cy/+ and healthy animals but there were no differences between the groups at all time points studied (Figure 2a). In addition, we detected stable FGF23 mRNA expression in spleen whereas no FGF23 mRNA expression was found in liver and heart tissue in both animal groups (results not shown). In polycystic kidneys increasing levels of FGF23 mRNA were detectable after 4 weeks. However, in healthy kidneys no FGF23 mRNA expression was detected (Figure 2a). FGF23 protein expression was detected by immunohistochemistry in cells lining the cysts in kidneys from cy/+ Han:SPRD rats but not in control kidneys (Figure 2b-f). Dmp1 and Fam20c modulate FGF23 expression in bone. We detected mRNA of both molecules in rat kidney at high levels. Fam20c expression was similar in cy/+ and control rats but Dmp1 expression was increased in kidneys from 8 weeks old cy/+ rats (Supplementary Figure 2).

$1,25(OH)_2$ vitamin D_3 metabolism

Plasma $1,25(OH)_2$ vitamin D_3 levels were similar among cy/+ and control animals at 2, 4, and 8 weeks (Figure 3a). In both groups $1,25(OH)_2$ vitamin D_3 levels decreased similarly over time. The relative mRNA expression of vitamin D receptor (VDR) is similar in both groups whereas there is a reduction of VDR from week 4 to 8 in cy/+ animals (Figure 3b). In addition, the relative mRNA expression of Cyp27b1 and Cyp24a1, the major enzymes responsible for vitamin D_3 metabolism was measured (Figures 3c and 3d). The mRNA expression of the catabolic enzyme Cyp24a1 was higher at 2 weeks in cy/+ animals. However, the expression of Cyp24a1 was

similar in cy/+ and +/+ animals after 4 and 8 weeks. For the anabolic enzyme Cyp27b1, we detected similar mRNA expression levels in the cy/+ and +/+ groups at all time points studied.

Renal phosphate and calcium handling

To evaluate the biological effect of high FGF23 plasma levels, we measured phosphate and calcium concentrations in blood and urine. The plasma phosphate and calcium levels as well as the renal excretion of calcium and phosphate were similar among cy/+ and +/+ animals at all time points studied (Figure 4).

Phosphate cotransporters NaPi-IIa and NaPi-IIc

The renal phosphate cotransporters NaPi-IIa and NaPi-IIc are downregulated by high levels of FGF23. In our study, the mRNA and protein expression levels of NaPi-IIa and NaPi-IIc were similar in both groups at 2, 4, and 8 weeks (Figures 5 and 6). Immunolocalization of NaPi-IIa protein in kidney sections of 4 and 8 weeks old cy/+ and +/+ animals demonstrated expression of NaPi-IIa protein in the brush border membrane of proximal tubules and smaller cysts as evident from colocalization with actin (Supplementary Figure 3). At these time points, basolateral NaPi-IIa staining was absent, whereas a prior report demonstrated aberrant NaPi-IIa localization in 32 weeks old Han:SPRD rats.[41]

Phosphate and glucose transport activities

We tested the sodium-dependent transport rate of ^{32}-labeled phosphate into brush border membrane vesicles in the absence and presence of phosphonoformic acid (PFA, 6 mM), an inhibitor of NaPi-IIa and NaPi-IIc, and found similar transport rates among cy/+ and control animals at 2 and 4 weeks (Figure 7). Na^+-dependent phosphate uptake in the absence of PFA was significantly increased in kidneys of 8

weeks old cy/+ rats. ^{3}H-glucose uptake was similar in both groups at all time points studied.

FGF23 and left ventricular hypertrophy (LVH)

High FGF23 plasma levels are associated with LVH.[42] We analyzed whether high FGF23 levels in 4 and 8 weeks old rats were associated with LVH but no difference was found for heart wall or septum thickness, heart to body weight or heart weight to tibia length (Supplementary Figure 4).

Klotho expression and FRS2a phosphorylation state

Since cy/+ animals appear to be resistant to the expected normal biological actions of FGF23 we examined whether Klotho availability or FGF23 signaling via the FGFR-1 receptor may be altered. We observed similar relative Klotho mRNA expression in cy/+ and +/+ animals at 2 and 4 weeks whereas at 8 weeks, Klotho mRNA expression was reduced in cy/+ animals (Figure 8a). Klotho protein abundance was similar in 8 weeks old cy/+ and +/+ animals (Figure 8b). Relative mRNA expression levels of FGFR-1 in kidney and bone were similar among cy/+ and +/+ animals (Supplementary Figure 5). The downstream signaling of FGF23, Klotho, and FGFR-1 complex leads to the phosphorylation of the FGF receptor substrate 2 alpha (FRS2a). Total FRS2a was similar in kidneys from 8 week old cy/+ and +/+ rats, whereas phosphorylated FRS2a protein was increased (Figure 8c).

Elevated plasma FGF23 and renal expression of FGF23 in conditional *Pkd1* KO mice

We employed a second model of PKD, the conditional *Pkd1* KO mice where deletion of *Pkd1* gene can be induced. We induced *Pkd1* deletion at days 15-19 after birth which result in a slow progression of cystic kidney disease.[43] Pkd1 mRNA was

strongly reduced in kidneys and bone from 10 week old *Pkd1*$^{fl/fl}$, cre+ mice as compared to *Pkd1*$^{fl/fl}$, cre- mice (Supplementary Figure 6). Conditional *Pkd1* KO elevated intact FGF23 plasma levels in 10 weeks old *Pkd1*$^{fl/fl}$, cre+ (277 ± 130 pg/ml) compared to *Pkd1*$^{fl/fl}$, cre- mice (199 ± 57 pg/ml) whereas TmP/GFR and creatinine clearance was similar in knockout and healthy animals (Figure 9). Intact PTH did not differ between *Pkd1*$^{fl/fl}$, cre+ (176 ± 71 pg/ml) and *Pkd1*$^{fl/fl}$, cre- (253±126 pg/ml) mice (Figure 9). Similar to the rat model, *Pkd1*$^{fl/fl}$, cre+ mice expressed similar FGF23 mRNA levels in bone as the control mice. Kidneys from *Pkd1*$^{fl/fl}$, cre+ mice expressed FGF23 mRNA and protein but not kidneys from *Pkd1*$^{fl/fl}$, cre- (Figure 10 and Supplementary Figure 7).

DISCUSSION

Our study provides four major findings: i) the Han:SPRD rat model accurately reproduces the observed increase of FGF23 levels in the early disease course of human ADPKD with normal kidney function, ii) Han:SPRD rats show resistance to highly elevated FGF23 levels as evident from normal phosphatemia, unchanged renal phosphate excretion, preserved expression of renal phosphate cotransporters, increased PTH, normal $1,25(OH)_2$ vitamin D_3 levels, and normal expression of Cyp27b1, iii) expression of FGF23 in polycystic kidneys, and iv) reproduction of the major findings in a second model of ADPKD, the inducible *Pkd1* KO mouse.

ADPKD patients with an estimated GFR of 60 ml/min/1.73m^2 and higher display strongly elevated FGF23 levels but only a small fraction of these patients present a reduction in renal phosphate reabsorption – albeit small – and a very mild hypophosphatemia.[31] In ADPKD patients with normal renal phosphate handling despite high FGF23 levels, reduced soluble Klotho levels were found whereas ADPKD patients that appeared to retain sensitivity to high FGF23 levels had preserved soluble Klotho levels.[32] However, the temporal sequence of rising FGF23 in PKD, the mechanisms underlying resistance to the biological actions of FGF23, and the source and cause of the elevated FGF23 levels remained unclear.

Herein, we demonstrate that intact FGF23 concentration in the cy/+ Han:SPRD rats increases early after birth before renal function decreases. The high FGF23 levels were accompanied by a 2-fold increase in PTH and normal $1,25(OH)_2$ vitamin D_3 levels. Plasma creatinine and urea indicated a decrease in renal function in cy/+ animals 6 weeks after birth and thereby 4 weeks after the rise in FGF23 and PTH.[35] Similarly, the inducible *Pkd1* KO mouse, a second ADPKD model, has elevated plasma FGF23 levels whereas creatinine clearance, TmP/GFR, and intact PTH

were normal. Thus, Han:SPRD rats and *Pkd1* KO mice illustrate an increase in FGF23 levels similar to that observed in young ADPKD patients with preserved renal function, thus allowing to approach the underlying mechanisms in more detail.

In healthy subjects and animals, a rise in FGF23 results in increased urinary excretion of phosphate through reduced expression of renal phosphate cotransporters, thus leading to a lowering of systemic serum phosphate concentrations; concomitant reduction in circulating levels of active $1,25(OH)_2$ vitamin D_3 levels occurs [44] which may participate in serum phosphate reduction.

ADPKD patients and the PKD rodent models are resistant to the elevated FGF23 as indicated by normophosphatemia, normal renal phosphate excretion, unchanged expression and activity of renal phosphate cotransporters, and apparently normal vitamin D_3 metabolism. Moreover, the expression and activity of the main renal phosphate cotransporters NaPi-IIa and NaPi-IIc are unchanged or elevated as indicated by immunoblotting, transport studies, and immunolocalization whereas in mice, overexpressing FGF23, NaPi-IIa mRNA and protein expressions are down regulated.[45] No left ventricular hypertrophy was detected suggesting either that FGF23 requires longer time periods, stronger elevation or that the heart is also resistant to high FGF23 levels.

Vitamin D_3 metabolism is similar in polycystic and control rats: indeed plasma $1,25(OH)_2$ vitamin D_3 concentrations and mRNA expression of Cyp27b1 did not differ between both groups of animals. Cyp24a1 was upregulated at 2 weeks in PKD animals which could be due to an early rise of plasma FGF23 concentration, but this effect was only transient and not observed at later time points.

We further investigated underlying mechanisms of resistance and found normal expression of the FGFR-1 receptor mediating the biological effects of FGF23 in the kidney.[14, 46] Mice constitutively expressing FGF23 have no changes in FGFR-1 expression levels suggesting that FGF23 per se does not modulate FGFR-1 expression.[45] Klotho is required to elicit FGF23 signals via the FGFR1 receptor.[14] In our PKD model Klotho protein abundance was unchanged. The activation of the Klotho/FGFR-1 complex leads to the phosphorylation of FRS2a. In the HanSPRD model pFRS2a was increased in cy/+ kidneys suggesting that FGF23 signaling can be induced but may be blocked further downstream.

PKD animals have also higher PTH levels than control animals which are in contrast to ADPDK patients with normal eGFR.[31] The elevation of PTH levels was also observed in other CKD rat models and may be due to the faster disease progression in animals compared with humans.[22, 24] Measurement of plasma PTH at shorter intervals or studies in another animal model with slower disease progression might overcome this gap. FGF23 suppresses PTH secretion in healthy rats but loss of Klotho expression in parathyroid glands may be involved in the induction of FGF23 resistance and secondary hyperparathyroidism.[47, 48]

We further analyzed the source(s) of elevated FGF23 by examining FGF23 mRNA expression in different organs such as bone as the major source of FGF23 in health, spleen, kidney, heart, and liver. In wildtype animals, we detected FGF23 mRNA expression mainly in bone, and very small amounts were also observed in spleen, whereas PKD rats and mice expressed FGF23 mRNA and protein also in the polycystic kidneys more precisely in the cells lining the cysts. In the rat and mouse PKD animal models FGF23 mRNA expression levels increased only in the polycystic kidneys whereas bone expressed similar mRNA levels in both groups suggesting that

kidney may be the major source of elevation of FGF23 levels in PKD. Similarly, in diabetic nephropathy the kidney may become a source of FGF23.[49] The mechanisms causing ectopic FGF23 expression in kidney are currently unknown. Interestingly, the kidney expresses several regulators of FGF23 secretion in bone such as Dmp1 and Fam20c and we found upregulation of Dmp1 in polycystic kidneys. In diabetic nephropathy, renal FGF23 expression was suppressed by ACE inhibition.[49] Several rodent models have been reported with elevated FGF23 levels induced by deletion of the OSR1 and SPAK protein kinases expressed in kidney.[50, 51] Whether these kinases contribute to elevated FGF23 levels in ADPKD models remains to be elucidated.

In summary, we found 10-fold elevated FGF23 levels in PKD animals and resistance of the target organs to its biological actions at early stage of polycystic kidney disease. The polycystic kidney may be a major source of FGF23 in this type of nephropathy.

METHODS

Animals

The Han:SPRD rat colony was established in our animal facility from a litter which was obtained from the Rat Resource and Research Center (Columbia, MO) [40]. Male heterozygous cystic (cy/+) and wild-type (+/+) rats were used in this study. *Pkd1* floxed/floxed (*Pkd1*$^{fl/fl}$) tamoxifen inducible cre mice were kindly provided by Gregory Germino.[52] Male and female *Pkd1*$^{fl/fl}$ cre+ and *Pkd* $^{fl/fl}$ cre- mice were used. We induced recombinase activity at days 15, 17, and 19 by injecting pups with 100 µl tamoxifen (2.5mg/ml) in corn oil. All animal studies were performed according to protocols approved by the legal authority (Veterinary Office of the Canton of Zurich).

Plasma and urine analysis

Blood and spot urine was collected from cy/+ and +/+ control rats at week 2, 4, 6, and 8 after birth. Some rats included in the week 6 group were sacrificed between 5 and 6 weeks after birth. Plasma and urine aliquots were rapidly frozen and stored at -80°C until measurement. Plasma concentrations of phosphate, calcium, and urea and urinary concentrations of phosphate and calcium were measured by the Institute of Clinical Chemistry at the University Hospital Zurich using standard methods. *Pkd1*$^{fl/fl}$ mice were fasted overnight before urine was collected for six hours in metabolic cages (Tecniplast®, Italy). Afterwards the mice were anesthetized with isoflurane and blood was collected from the heart. Urine and plasma laboratory analysis were performed by the Zurich Integrative Rodent Physiology (ZIRP) core facility.

The ratio of the maximum rate of tubular phosphate reabsorption to the glomerular filtration rate (TmP/GFR) was calculated as follows:

TmP/GFR in mmol/L = P_P - [U_P x P_{crea} / U_{crea}]

where P_P, U_P, P_{crea} , and U_{crea} refer to the plasma and urinary concentration of phosphate and creatinine, respectively.[53] The fractional excretion of calcium was calculated according to the following equation:

FECa = (U_{Ca} x P_{crea})/(PCa x U_{crea}) x 100

where P_{Ca}, U_{Ca}, P_{crea}, and U_{crea} refer to the plasma and urinary concentrations of calcium and creatinine, respectively.

The plasma concentration of intact FGF23 (Kainos Laboratories, Tokyo, Japan), intact PTH (Immutopics International, California, USA) and 1,25$(OH)_2$ vitamin D_3 (Immunodiagnostic Systems, London, UK) were measured by enzyme-linked immunosorbent assays according to the manufacturer's protocols.

RNA extraction and RT-PCR

Rats were sacrificed at week 2, 4, and 8 for harvesting kidney, bone, liver, spleen, and heart. Mice were sacrificed at week 10 for harvesting kidneys and bone. The organs were rapidly frozen in liquid nitrogen. Total RNA was extracted using the Qiagen RNeasy Mini Kit (Qiagen, Hombrechtikon, Switzerland) or TRizol reagent for bone tissue (Invitrogen, Zug, Switzerland). Snap-frozen tissue slices were homogenized in a pestle homogenizer (Potter-Elvehjem type) together with 1ml precooled RLT-Buffer supplemented with β-mercaptoethanol at a final concentration of 1%. Subsequently, 700 µl of the homogenate were used for RNA preparation, which was carried out according to the manufacturer's protocol. DNAse digestion was performed using the RNase-free DNAase Set (Qiagen; Hilden, Germany). Total RNA extractions were analyzed for quality, purity, and concentration using the NanoDrop ND-1000 spectrophotometer (Wilmington, DE, USA). RNA samples were diluted to a final con-

centration of 100 ng/µl and cDNA was prepared using the TaqMan Reverse Transcriptase Reagent Kit (Applied Biosystems, Roche; Forster City, CA, USA).

In brief, in a reaction volume of 40 µl, 300 ng of RNA was used as template and mixed with the following final concentrations of RT buffer (1x), $MgCl_2$ (5.5 mM), random hexamers (2.5 µM), dNTP mix (500 µM each), RNase inhibitor (0.4 U/µl), multiscribe reverse transcriptase (1.25 U/µl) and RNAse-free water. Reverse transcription was performed with thermocycling conditions set at 25°C for 10 min, 48°C for 30 min, and 95°C for 5 min on a thermocyler (Biometra, Goettingen, Germany).

Quantitative real-time PCR (qRT-PCR) was performed on the ABI PRISM 7700 Sequence Detection System (Applied Biosystems). Primers for all genes of interest (Supplementary Table 1) were designed using Primer Express software from Applied Biosystems. Primers were chosen to result in amplicons no longer than 150 bp spanning intron-exon boundaries to exclude genomic DNA contamination. The specificity of all primers was first tested on mRNA derived from kidney, bone or intestine and always resulted in a single product of the expected size (data not shown). Probes were labelled with the reporter dye FAM at the 5'-end and the quencher dye TAMRA at the 3'-end (Microsynth, Balgach, Switzerland). Real-Time PCR reactions were performed using TaqMan Universal PCR Master Mix (Applied Biosystems) as described [10].

^{32}P and ^{3}H-glucose-uptake in brush border membrane vesicles

Brush border membrane vesicles were prepared using the Mg^{2+}-precipitation technique [54, 55] and further used for western blotting and transport studies. The transport rate of ^{32}-labeled phosphate and tritium labeled glucose into renal brush border membrane vesicles was determined at 30s and 120min (equilibrium value) as

described [54] at 25°C in the presence of inward gradients of 100 mM NaCl or 100 mM KCl and 0.1 mM K_2HPO_4. All measurements were performed in triplicates.

Western blot analysis

After measurement of the protein concentration (Bio-Rad, Hercules, CA), 10 µg of renal brush border membrane for NaPi-IIa and NaPi-IIc and 20 µg or 2 µg, respectively, of total kidney homogenate for FRS2a/pFRS2a and Klotho was solubilized in loading buffer containing DTT and separated on 8% polyacrylamide gels. For immunoblotting, proteins were transferred electrophoretically to polyvinylidene fluoride membranes (Immobilon-P, Millipore, Bedford, MA, USA). After blocking with 5% milk powder in Tris-buffered saline/0.1% Tween-20 for 60min, blots were incubated with the primary antibodies: rabbit polyclonal anti-NaPi-IIa (1:6000),[56, 57] rabbit polyclonal anti-NaPi-IIc (1:10000),[10] mouse monoclonal anti-β-actin antibody (42kD; Sigma, St. Louis, MO; 1:5000), mouse monoclonal anti-FRS2a (R&D Systems, USA; 1:1500), rabbit polyclonal anti-pFRS2a (Cell Signaling Technology, USA; 1:2000), rat monoclonal anti-Klotho (Clone KM2076, TransGenic Inc., Japan; 1:1000) and mouse monoclonal anti-GAPDH (Merck Millipore, USA; 1:20000) either for 2h at room temperature or overnight at 4°C. Membranes were then incubated for 1h at room temperature with secondary goat anti-rabbit, donkey anti-mouse or goat anti-rat antibodies (1:5000) linked to alkaline phosphatase (Promega, USA), HRP (Amersham, USA or R&D Systems, USA). The protein signal was detected with the appropriate substrates using the DIANA III-chemiluminescence detection system (Raytest, Straubenhardt, Germany). All images were analyzed using the software Advanced Image Data Analyser AIDA, Raytest to calculate the protein of interest/actin ratio.

Immunofluorescence staining

Rat kidneys were perfused in situ through the left heart ventricle with a fixative solution containing 3% paraformaldehyde in phosphate buffered saline (PBS). Mouse kidneys were immersed in a fixative solution containing formalin (10%). Kidneys were embedded in TissueTec and frozen in liquid nitrogen cooled by liquid propane. Five µm cryosections were cut. Slides were washed in PBS and incubated in 50 mM NH_4Cl in PBS for 20 min at room temperature to reduce free aldehyde groups. For FGF23 staining, slides were treated for 5 min with 0.5% SDS in PBS. Unspecific sites were blocked with 1% bovine serum albumin (BSA) in PBS for 1h at room temperature. Primary antibodies were diluted in 1% BSA in PBS (NaPi-IIa 1:1000; anti-FGF23 (R&D Systems, USA) 1:1000; anti-Calbindin (Swant, Switzerland) 1:20000) and kidney sections were incubated with the primary antibody over night at 4°C. After washing with PBS, sections were incubated with the corresponding secondary antibody (1:500) (anti-rabbit Alexa594 (Invitrogen, Switzerland), anti-rat NL493 (R&D Systems, USA); anti-mouse (DyLight 649, Jackson ImmunoResearch, Europe), phalloidin-FITC (1:200), and DAPI (Invitrogen,1:1000) for 1h at room temperature. Slides were washed twice with PBS before being mounted with Dako glycergel mounting medium. Sections were visualised on a Leica DM 5500B fluorescence microscope and images processed with Adobe Photoshop CS5 extended.

Statistical analysis

Statistics were performed using unpaired Student's t-test (GraphPad Prism version 5.0, GraphPad, San Diego, CA). Random-effects models for longitudinal data were applied to analyse unbalanced repeated measures (SAS version 9.3, Cary, NC, USA). Data are provided as mean ± SD. $P < 0.05$ was considered significant.

DISCLOSURE

All authors declared no competing interests.

ACKNOWLEDGEMENTS

This study was supported by grants from the Swiss National Science Foundation (No. 310000-118166) to A. Serra, the Swiss National Center for Competence in Research Kidney. CH to C. A. Wagner., and by a collaborative grant from the Zurich Center for Integrative Human Physiology (ZIHP) to J. Biber, A. Serra, and C. A. Wagner, H. Zhang. was partly supported by a doctoral scholarship from the China Scholarship Council (CSC). S. Segerer is supported by grants from the CKM and the Hartmann Müller-Stiftung. The use of the ZIRP Core facility for Rodent Physiology is gratefully acknowledged. We thank O. Devuyst for helpful comments.

TITLES AND LEGENDS

Figure 1

FGF23, PTH and renal function. Plasma concentrations of FGF23 (a), PTH (b), creatinine (c) and urea (d) after 2, 4, 6, and 8 weeks in cy/+ (black squares) and +/+ (white squares) Han:SPRD rats (mean ±SD); number of animals (median), cy/+ = 11.5, +/+ = 11; * $p<0.05$ and ** $p<0.001$

Figure 2

FGF23 expression in kidney. (a) Relative mRNA expression of FGF23 to 18S rRNA in bone and kidney after 2, 4, and 8 weeks in cy/+ (black bars) and +/+ (white bars) Han:SPRD rats (mean ±SD); number of animals (median), cy/+ = 6, +/+ = 5.5; ** $p<0.001$. Immunohistochemistry for FGF23 (green), calbindin D28k (red), a marker for distal convoluted tubules and connecting tubules, and DAPI (blue, cell nuclei): (b,c) kidneys from 8 week old cy/+ rats, (d,e) kidneys from 8 week old control rats, (f) kidney from 8 week old cy/+ rat incubated with secondary antibodies alone. Original magnification 400 x.

Figure 3

Vitamin D_3 metabolism. Plasma concentration of $1,25(OH)_2$ Vitamin D_3 (a), relative mRNA expression of the vitamin D receptor (VDR) (b) as well as Cyp27b1 (c) and Cyp24a1 (d) enzymes in the kidney to 18S rRNA after 2, 4, and 8 weeks in cy/+ (black bars) and +/+ (white bars) Han:SPRD rats (mean ±SD); number of animals (median), cy/+ = 6, +/+ = 5; * $p<0.05$ and ** $p<0.001$.

Figure 4

Renal phosphate and calcium handling. Plasma concentrations of phosphate (a) and calcium (b) as well as TmP/GFR (c) and FECa ratio (d) after 2, 4, 6, and 8 weeks in cy/+ (black squares) and +/+ (white squares) Han:SPRD rats (mean ±SD); number of animals (median), cy/+ = 11.5, +/+ =11; * $p<0.05$.

Figure 5

Phosphate transporter mRNA expression. Relative mRNA expression of NaPi-IIa (a) and NaPi-IIc (b) to 18S rRNA after 2, 4, and 8 weeks in cy/+ (black bars) and +/+ (white bars) Han:SPRD rats (mean ±SD); number of animals (median), cy/+ = 6, +/+ = 6; * $p<0.05$.

Figure 6

Phosphate transporter protein expression. Relative protein expression of NaPi-IIa and NaPi-IIc to β-actin after 2 (a), 4 (b), and 8 (c) weeks in cy/+ (black bars) and +/+ (white bars) Han:SPRD rats (mean ±SD); number of animals (median), cy/+ = 6, +/+ = 6; * $p<0.05$.

Figure 7

Phosphate and glucose uptake into renal brush border membrane vesicles. Phosphate uptake without (a) and with (b) PFA and glucose uptake (c) after 2, 4, and 8 weeks in cy/+ (black bars) and +/+ (white bars) Han:SPRD rats (mean ±SD); number of animals (median), cy/+ = 11, +/+ = 7; * $p<0.05$.

Figure 8

Klotho expression and phosphorylation state of FRS2a. Relative mRNA expression of Klotho in kidney (a) to 18S rRNA after 2, 4, and 8 weeks; relative protein expression of Klotho (b) and phosphorylation state of FRS2a (c) to GAPDH after 8 weeks in cy/+ (black bars) and +/+ (white bars) Han:SPRD rats (mean ±SD); number of animals (median), cy/+ = 4, +/+ = 4; * $p<0.05$.

Figure 9

FGF23, PTH, TmP/GFR, and renal function in *Pkd1*$^{fl/fl}$ mice. Plasma intact FGF23 (a) and PTH (b) as well as TmP/GFR (c) and creatinine clearance (d) after 10 weeks in *Pkd1*$^{fl/fl}$, cre+ (black bars) and *Pkd1*$^{fl/fl}$, cre- (white bars) mice (mean ±SD); number of animals (median), *Pkd1*$^{fl/fl}$, cre+ = 7, *Pkd1*$^{fl/fl}$, cre- = 16; * $p<0.05$.

Figure 10

FGF23 and Klotho expression in bone and kidneys of *Pkd1*$^{fl/fl}$ mice.
Relative mRNA expression of FGF23 in kidney (a) and bone (b) as well as Klotho in kidney (c) to 18S rRNA after 10 weeks in *Pkd1*$^{fl/fl}$, cre+ (black bars) and *Pkd1*$^{fl/fl}$, cre- (white bars) mice (mean ±SD), *Pkd1*$^{fl/fl}$, cre+ = 8, *Pkd1*$^{fl/fl}$, cre- = 15 * $p<0.05$ and ** $p<0.001$.

REFERENCES

[1] Bacic D, Capuano P, Baum M, *et al.* Activation of dopamine D1-like receptors induces acute internalization of the renal Na+/phosphate cotransporter NaPi-IIa in mouse kidney and OK cells. *Am J Physiol Renal Physiol* 2005; **288**: F740–F747.

[2] Bacic D, Lehir M, Biber J, *et al.* The renal Na+/phosphate cotransporter NaPi-IIa is internalized via the receptor-mediated endocytic route in response to parathyroid hormone. *Kidney Int* 2006; **69**: 495–503.

[3] Baum M, Schiavi S, Dwarakanath V, *et al.* Effect of fibroblast growth factor-23 on phosphate transport in proximal tubules. *Kidney Int* 2005; **68**: 1148–1153.

[4] Berndt T J, Bielesz B, Craig T A, *et al.* Secreted frizzled-related protein-4 reduces sodium-phosphate co-transporter abundance and activity in proximal tubule cells. *Pflugers Arch* 2006; **451**: 579–587.

[5] Biber J, Hernando N, Forster I, *et al.* Regulation of phosphate transport in proximal tubules. *Pflugers Arch* 2009; **458**: 39–52.

[6] Capuano P, Radanovic T, Wagner C A, *et al.* Intestinal and renal adaptation to a low-Pi diet of type II NaPi cotransporters in vitamin D receptor- and 1alphaOHase-deficient mice. *Am J Physiol Cell Physiol* 2005; **288**: C429–C434.

[7] Murer H, Hernando N, Forster I, *et al.* Proximal tubular phosphate reabsorption: molecular mechanisms. *Physiol Rev* 2000; **80**: 1373–1409.

[8] Murer H, Hernando N, Forster I, *et al.* Regulation of Na/Pi transporter in the proximal tubule. *Annu Rev Physiol* 2003; **65**: 531–542.

[9] Picard N, Capuano P, Stange G, *et al.* Acute parathyroid hormone differentially regulates renal brush border membrane phosphate cotransporters. *Pflugers Arch* 2010; **460**: 677–687.

[10] Nowik M, Lecca M R, Velic A, *et al.* Genome-wide gene expression profiling reveals renal genes regulated during metabolic acidosis. *Physiol Genomics* 2008; **32**: 322–334.

[11] Yamashita T, Yoshioka M, Itoh N. Identification of a novel fibroblast growth factor, FGF-23, preferentially expressed in the ventrolateral thalamic nucleus of the brain. *Biochem Biophys Res Commun* 2000; **277**: 494–498.

[12] Liu S, Guo R, Simpson L G, *et al.* Regulation of fibroblastic growth factor 23 expression but not degradation by PHEX. *J Biol Chem* 2003; **278**: 37419–37426.

[13] Shimada T, Hasegawa H, Yamazaki Y, *et al.* FGF-23 is a potent regulator of vitamin D metabolism and phosphate homeostasis. *J Bone Miner Res* 2004; **19**: 429–435.

[14] Urakawa I, Yamazaki Y, Shimada T, *et al.* Klotho converts canonical FGF receptor into a specific receptor for FGF23. *Nature* 2006; **444**: 770–774.

[15] Farrow E G, Davis S I, Summers L J, *et al.* Initial FGF23-mediated signaling occurs in the distal convoluted tubule. *J Am Soc Nephrol* 2009; **20**: 955–960.

[16] Olauson H, Lindberg K, Amin R, *et al.* Targeted deletion of klotho in kidney distal tubule disrupts mineral metabolism. *J Am Soc Nephrol* 2012; **23**: 1641–1651.

[17] Andrukhova O, Zeitz U, Goetz R, *et al.* FGF23 acts directly on renal proximal tubules to induce phosphaturia through activation of the ERK1/2-SGK1 signaling pathway. *Bone* 2012; **51**: 621–628.

[18] Block G A, Klassen P S, Lazarus J M, *et al.* Mineral metabolism, mortality, and morbidity in maintenance hemodialysis. *J Am Soc Nephrol* 2004; **15**: 2208–2218.

[19] Shigematsu T, Kazama J J, Yamashita T, *et al.* Possible involvement of circulating fibroblast growth factor 23 in the development of secondary hyperparathyroidism associated with renal insufficiency. *Am J Kidney Dis* 2004; **44**: 250–256.

[20] Gutierrez O, Isakova T, Rhee E, *et al.* Fibroblast growth factor-23 mitigates hyperphosphatemia but accentuates calcitriol deficiency in chronic kidney disease. *J Am Soc Nephrol* 2005; **16**: 2205–2215.

[21] Evenepoel P, Meijers B, Viaene L, *et al.* Fibroblast growth factor-23 in early chronic kidney disease: additional support in favor of a phosphate-centric paradigm for the pathogenesis of secondary hyperparathyroidism. *Clin J Am Soc Nephrol* 2010; **5**: 1268–1276.

[22] Isakova T, Wahl P, Vargas G S, *et al.* Fibroblast growth factor 23 is elevated before parathyroid hormone and phosphate in chronic kidney disease. *Kidney Int* 2011; **79**: 1370–1378.

[23] Pavik I, Jaeger P, Ebner L, *et al.* Secreted Klotho and FGF23 in chronic kidney disease Stage 1 to 5: a sequence suggested from a cross-sectional study. *Nephrol Dial Transplant* 2013; **28**: 352–359.

[24] Hasegawa H, Nagano N, Urakawa I, *et al.* Direct evidence for a causative role of FGF23 in the abnormal renal phosphate handling and vitamin D metabolism in rats with early-stage chronic kidney disease. *Kidney Int* 2010; **78**: 975–980.

[25] Torres V E, Harris P C, Pirson Y. Autosomal dominant polycystic kidney disease. *Lancet* 2007; **369**: 1287–1301.

[26] Reeders S T, Breuning M H, Davies K E, *et al.* A highly polymorphic DNA marker linked to adult polycystic kidney disease on chromosome 16. *Nature* 1985; **317**: 542–544.

[27] Peters D J, Spruit L, Saris J J, *et al.* Chromosome 4 localization of a second gene for autosomal dominant polycystic kidney disease. *Nat Genet* 1993; **5**: 359–362.

[28] Kimberling W J, Kumar S, Gabow P A, *et al.* Autosomal dominant polycystic kidney disease: localization of the second gene to chromosome 4q13-q23. *Genomics* 1993; **18**: 467–472.

[29] Hughes J, Ward C J, Peral B, *et al.* The polycystic kidney disease 1 (PKD1) gene encodes a novel protein with multiple cell recognition domains. *Nat Genet* 1995; **10**: 151–160.

[30] Mochizuki T, Wu G, Hayashi T, *et al.* PKD2, a gene for polycystic kidney disease that encodes an integral membrane protein. *Science* 1996; **272**: 1339–1342.

[31] Pavik I, Jaeger P, Kistler A D, *et al.* Patients with autosomal dominant polycystic kidney disease have elevated fibroblast growth factor 23 levels and a renal leak of phosphate. *Kidney Int* 2011; **79**: 234–240.

[32] Pavik I, Jaeger P, Ebner L, *et al.* Soluble klotho and autosomal dominant polycystic kidney disease. *Clin J Am Soc Nephrol* 2012; **7**: 248–257.

[33] Bihoreau M T, Ceccherini I, Browne J, *et al.* Location of the first genetic locus, PKDr1, controlling autosomal dominant polycystic kidney disease in Han:SPRD cy/+ rat. *Hum Mol Genet* 1997; **6**: 609–613.

[34] Brown J H, Bihoreau M T, Hoffmann S, *et al.* Missense mutation in sterile alpha motif of novel protein SamCystin is associated with polycystic kidney disease in (cy/+) rat. *J Am Soc Nephrol* 2005; **16**: 3517–3526.

[35] Schäfer K, Gretz N, Bader M, *et al.* Characterization of the Han:SPRD rat model for hereditary polycystic kidney disease. *Kidney Int* 1994; **46**: 134–152.

[36] Ahrabi A K, Jouret F, Marbaix E, *et al.* Glomerular and proximal tubule cysts as early manifestations of Pkd1 deletion. *Nephrol Dial Transplant* 2010; **25**: 1067–1078.

[37] Torres V E, Bengal R J, Litwiller R D, *et al.* Aggravation of polycystic kidney disease in Han:SPRD rats by buthionine sulfoximine. *J Am Soc Nephrol* 1997; **8**: 1283–1291.

[38] Turner C M, Ramesh B, Srai S K S, *et al.* Altered ATP-sensitive P2 receptor subtype expression in the Han:SPRD cy/+ rat, a model of autosomal dominant polycystic kidney disease. *Cells Tissues Organs* 2004; **178**: 168–179.

[39] Wahl P R, Serra A L, Le Hir M, *et al.* Inhibition of mTOR with sirolimus slows disease progression in Han:SPRD rats with autosomal dominant polycystic kidney disease (ADPKD). *Nephrol Dial Transplant* 2006; **21**: 598–604.

[40] Wu M, Arcaro A, Varga Z, *et al.* Pulse mTOR inhibitor treatment effectively controls cyst growth but leads to severe parenchymal and glomerular hypertrophy in rat polycystic kidney disease. *Am J Physiol Renal Physiol* 2009; **297**: F1597–F1605.

[41] Vogel M, Kränzlin B, Biber J, *et al.* Altered expression of type II sodium/phosphate cotransporter in polycystic kidney disease. *J Am Soc Nephrol* 2000; **11**: 1926–1932.

[42] Faul C, Amaral A P, Oskouei B, *et al.* FGF23 induces left ventricular hypertrophy. *J Clin Invest* 2011; **121**: 4393–4408.

[43] Piontek K, Menezes L F, Garcia-Gonzalez M A, *et al.* A critical developmental switch defines the kinetics of kidney cyst formation after loss of Pkd1. *Nat Med* 2007; **13**: 1490–1495.

[44] Bergwitz C, Jüppner H. Regulation of phosphate homeostasis by PTH, vitamin D, and FGF23. *Annu Rev Med* 2010; **61**: 91–104.

[45] Marsell R, Krajisnik T, Göransson H, *et al.* Gene expression analysis of kidneys from transgenic mice expressing fibroblast growth factor-23. *Nephrol Dial Transplant* 2008; **23**: 827–833.

[46] Liu S, Vierthaler L, Tang W, *et al.* FGFR3 and FGFR4 do not mediate renal effects of FGF23. *J Am Soc Nephrol* 2008; **19**: 2342–2350.

[47] Ben-Dov I Z, Galitzer H, Lavi-Moshayoff V, *et al.* The parathyroid is a target organ for FGF23 in rats. *J Clin Invest* 2007; **117**: 4003–4008.

[48] Galitzer H, Ben-Dov I Z, Silver J, *et al.* Parathyroid cell resistance to fibroblast growth factor 23 in secondary hyperparathyroidism of chronic kidney disease. *Kidney Int* 2010; **77**: 211–218.

[49] Zanchi C, Locatelli M, Benigni A, *et al.* Renal Expression of FGF23 in Progressive Renal Disease of Diabetes and the Effect of Ace Inhibitor. *PLoS One* 2013; **8**: e70775.

[50] Pathare G, Föller M, Michael D, *et al.* Enhanced FGF23 serum concentrations and phosphaturia in gene targeted mice expressing WNK-resistant SPAK. *Kidney Blood Press Res* 2012; **36**: 355–364.

1 [51] Pathare G, Föller M, Daryadel A, *et al.* OSR1-sensitive renal tubular phos-
2 phate reabsorption. *Kidney Blood Press Res* 2012; **36**: 149–161.

3 [52] Piontek K B, Huso D L, Grinberg A, *et al.* A functional floxed allele of Pkd1 that
4 can be conditionally inactivated in vivo. *J Am Soc Nephrol* 2004; **15**: 3035–3043.

5 [53] Brodehl J, Krause A, Hoyer P F. Assessment of maximal tubular phosphate
6 reabsorption: comparison of direct measurement with the nomogram of Bijvoet.
7 *Pediatr Nephrol* 1988; **2**: 183–189.

8 [54] Biber J, Stieger B, Haase W, *et al.* A high yield preparation for rat kidney brush
9 border membranes. Different behaviour of lysosomal markers. *Biochim Biophys Acta*
10 1981; **647**: 169–176.

11 [55] Biber J, Stieger B, Stange G, *et al.* Isolation of renal proximal tubular brush-
12 border membranes. *Nat Protoc* 2007; **2**: 1356–1359.

13 [56] Custer M, Lötscher M, Biber J, *et al.* Expression of Na-P(i) cotransport in rat
14 kidney: localization by RT-PCR and immunohistochemistry. *Am J Physiol* 1994; **266**:
15 F767–F774.

16 [57] Hilfiker H, Hattenhauer O, Traebert M, *et al.* Characterization of a murine type
17 II sodium-phosphate cotransporter expressed in mammalian small intestine. *Proc*
18 *Natl Acad Sci U S A* 1998; **95**: 14564–14569.

19

Figure 1

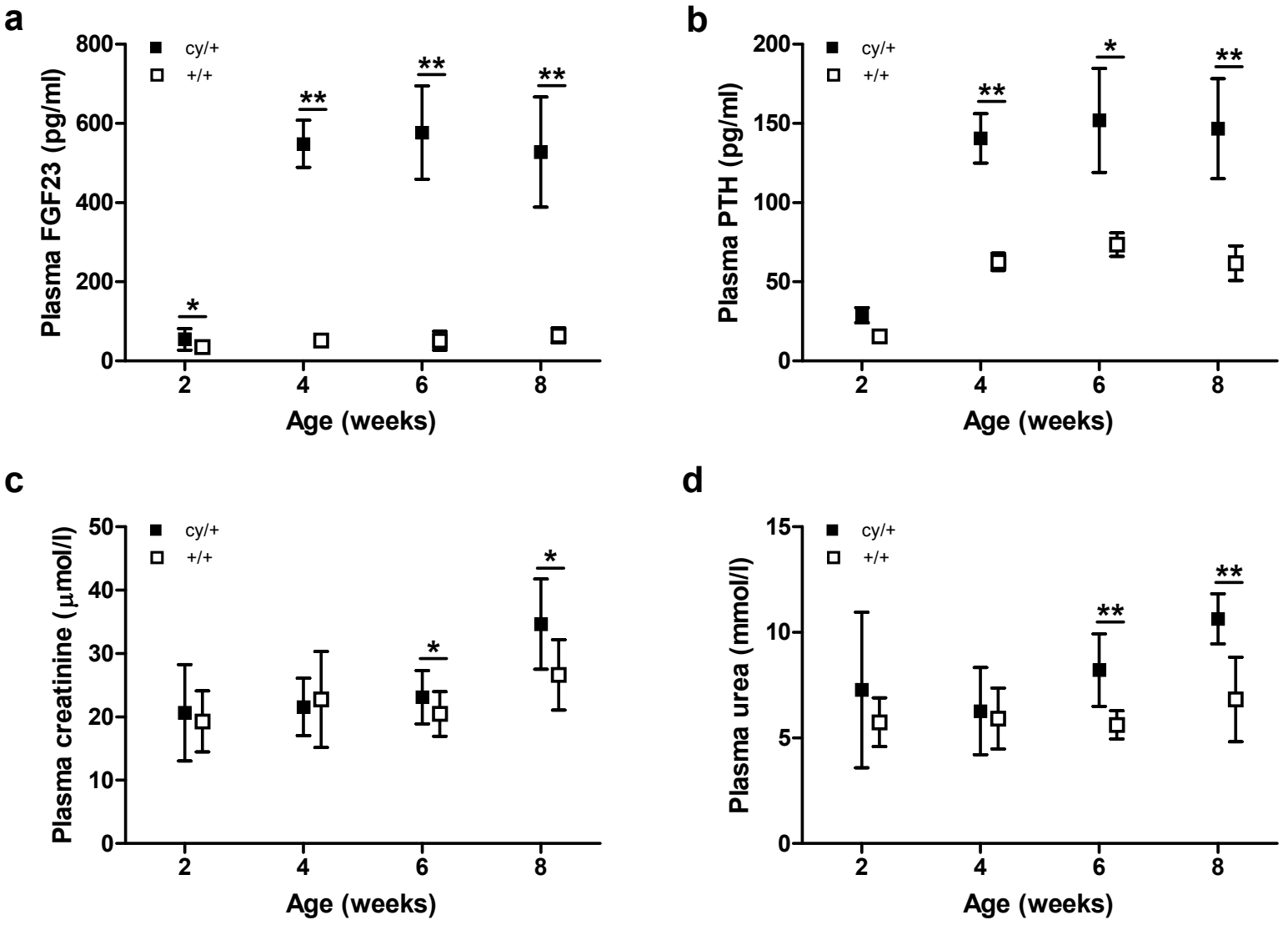
a
Plasma FGF23 (pg/ml)
800
600
400
200
0
cy/+
+/+
**
**
**
*
2
4
6
8
Age (weeks)
b
Plasma PTH (pg/ml)
200
150
100
50
0
cy/+
+/+
**
*
**
2
4
6
8
Age (weeks)
c
Plasma creatinine (μmol/l)
50
40
30
20
10
0
cy/+
+/+
*
*
2
4
6
8
Age (weeks)
d
Plasma urea (mmol/l)
15
10
5
0
cy/+
+/+
**
**
2
4
6
8
Age (weeks)

Figure 2

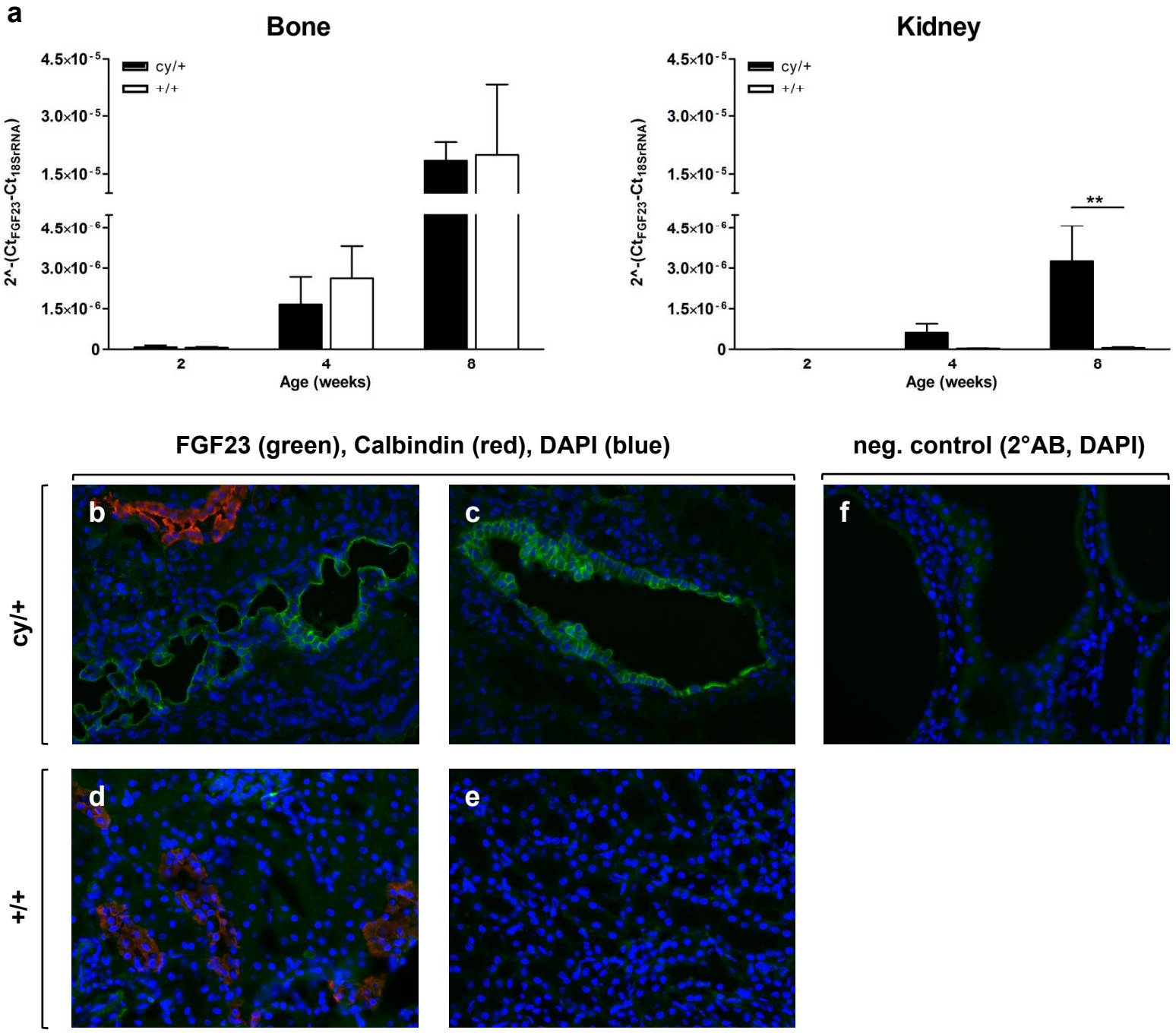
a
Bone
Kidney
cy/+
+/+
2^-(Ct_FGF23-Ct_18SrRNA)
4.5x10^-5
3.0x10^-5
1.5x10^-5
4.5x10^-6
3.0x10^-6
1.5x10^-6
0
2
4
8
Age (weeks)
**
FGF23 (green), Calbindin (red), DAPI (blue)
neg. control (2°AB, DAPI)
b
c
d
e
f

Figure 3

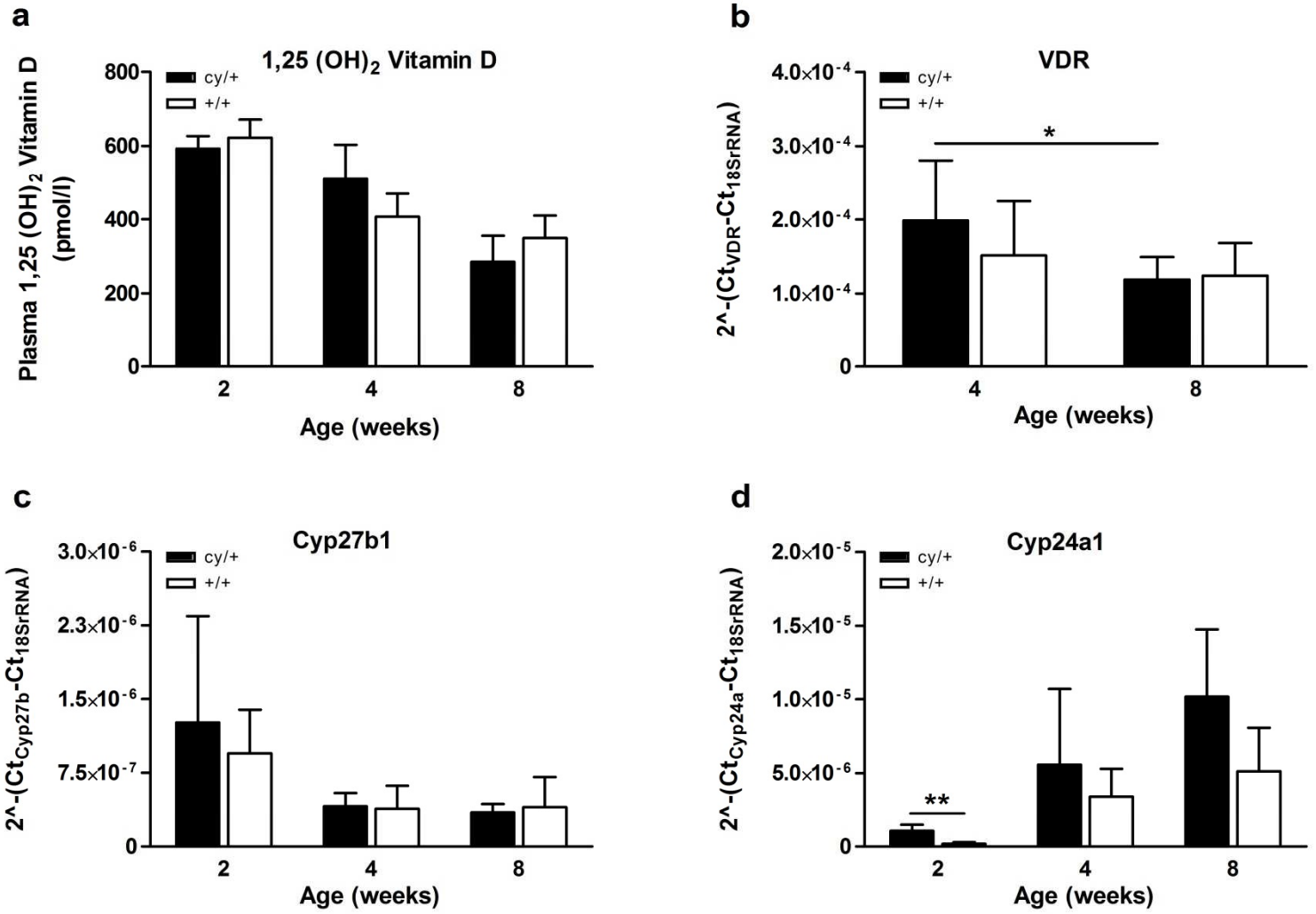
a
1,25 (OH)2 Vitamin D
Plasma 1,25 (OH)2 Vitamin D (pmol/l)
cy/+
+/+
800
600
400
200
0
2
4
8
Age (weeks)
b
VDR
2^-(CtVDR-Ct18SrRNA)
4.0×10-4
3.0×10-4
2.0×10-4
1.0×10-4
0
*
4
8
Age (weeks)
c
Cyp27b1
2^-(CtCyp27b-Ct18SrRNA)
3.0×10-6
2.3×10-6
1.5×10-6
7.5×10-7
0
2
4
8
Age (weeks)
d
Cyp24a1
2^-(CtCyp24a-Ct18SrRNA)
2.0×10-5
1.5×10-5
1.0×10-5
5.0×10-6
0
**
2
4
8
Age (weeks)

Figure 4

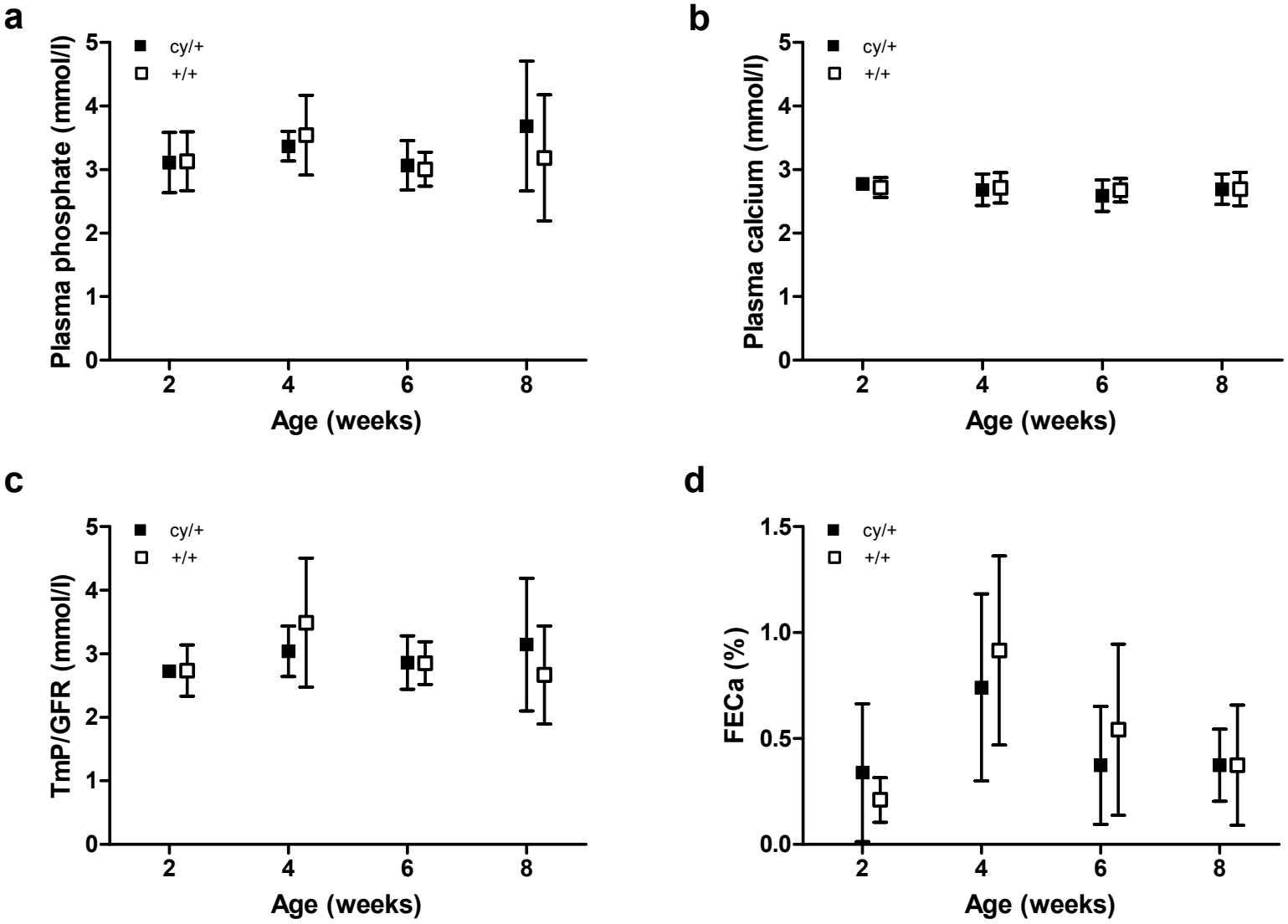
a
Plasma phosphate (mmol/l)
cy/+
+/+
Age (weeks)
b
Plasma calcium (mmol/l)
cy/+
+/+
Age (weeks)
c
TmP/GFR (mmol/l)
cy/+
+/+
Age (weeks)
d
FECa (%)
cy/+
+/+
Age (weeks)

Figure 5

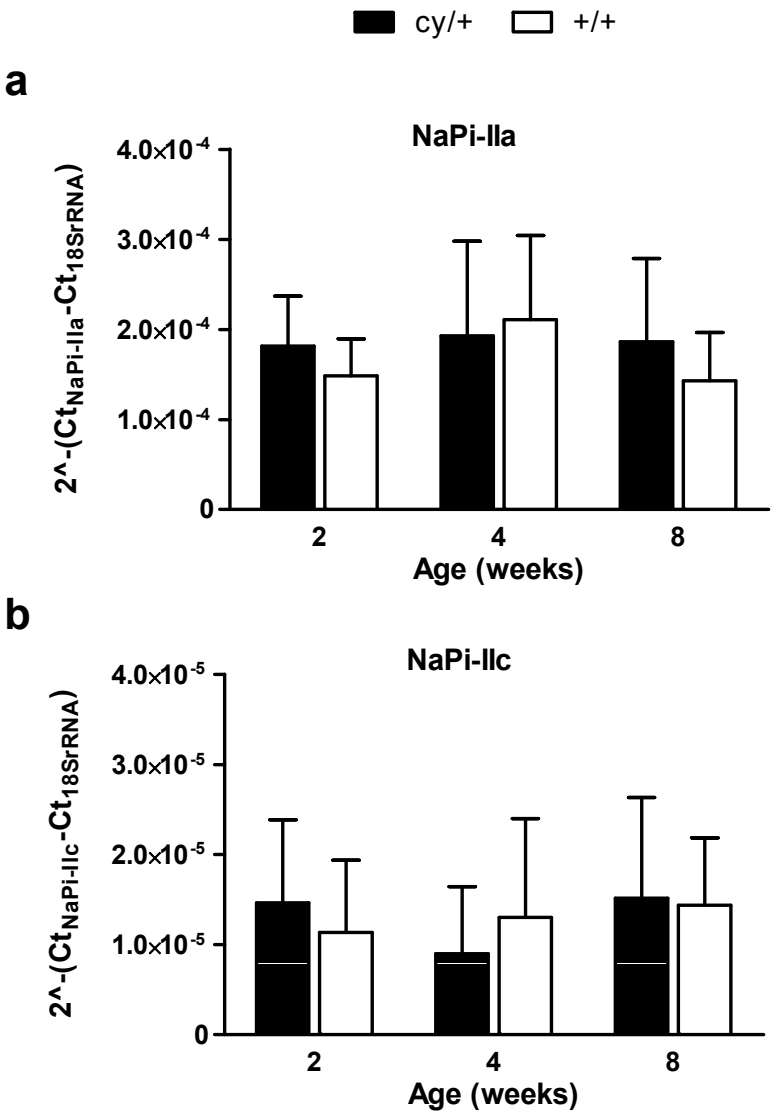
cy/+
+/+
a
NaPi-IIa
4.0×10-4
3.0×10-4
2.0×10-4
1.0×10-4
0
2^-(CtNaPi-IIa-Ct18SrRNA)
2
4
8
Age (weeks)
b
NaPi-IIc
4.0×10-5
3.0×10-5
2.0×10-5
1.0×10-5
0
2^-(CtNaPi-IIc-Ct18SrRNA)
2
4
8
Age (weeks)

Figure 6

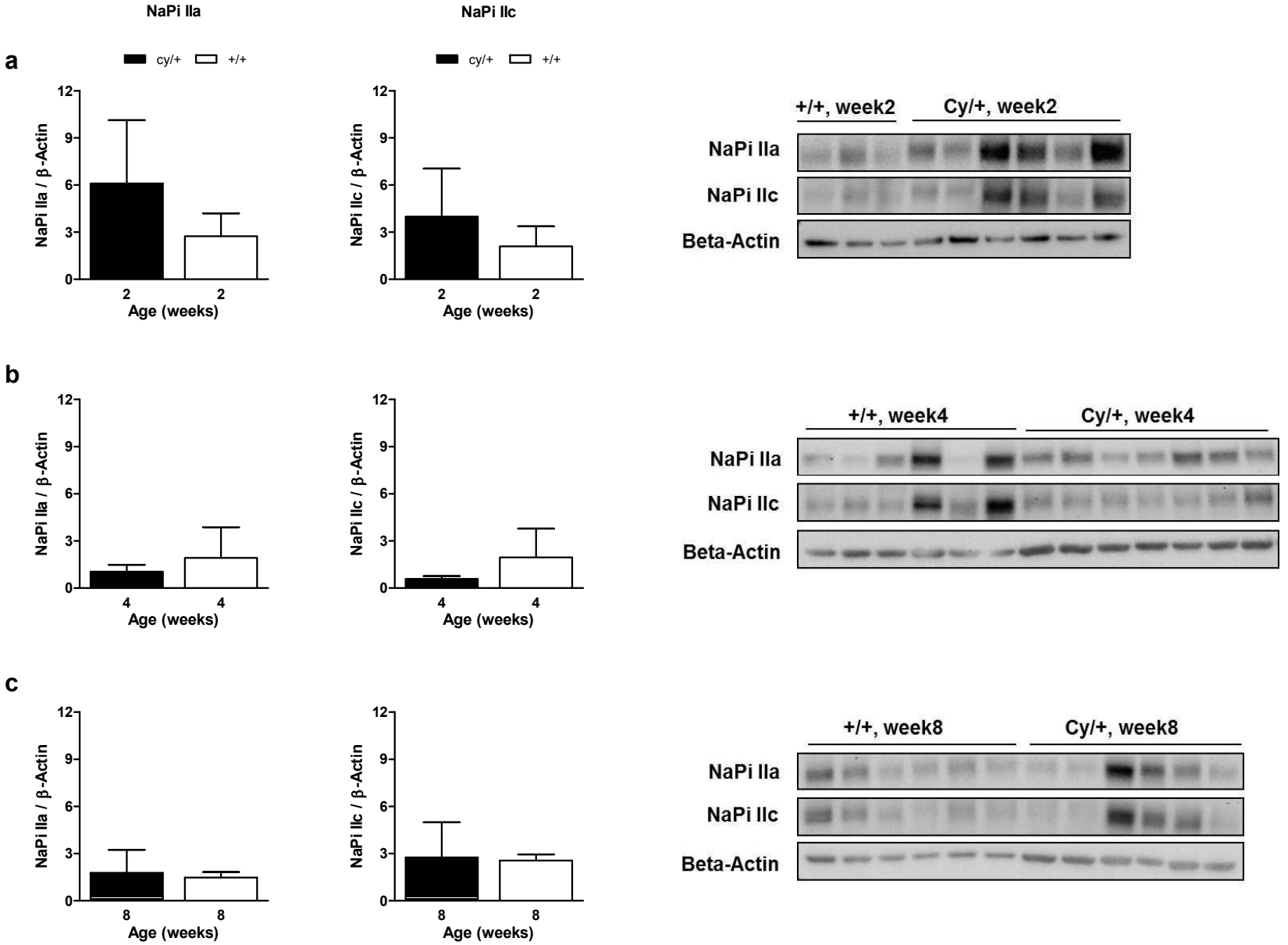
NaPi IIa
NaPi IIc
a
cy/+
+/+
NaPi IIa / β-Actin
NaPi IIc / β-Actin
12
9
6
3
0
2
2
Age (weeks)
+/+, week2
Cy/+, week2
NaPi IIa
NaPi IIc
Beta-Actin
b
4
4
Age (weeks)
+/+, week4
Cy/+, week4
c
8
8
Age (weeks)
+/+, week8
Cy/+, week8

Figure 7

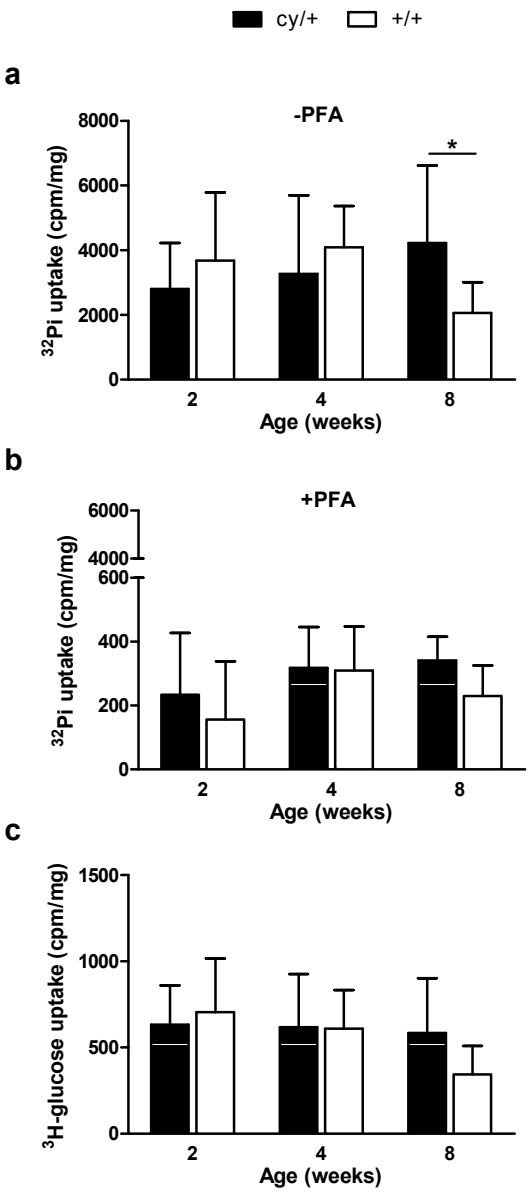
cy/+
+/+
a
-PFA
^{32}Pi uptake (cpm/mg)
8000
6000
4000
2000
0
*
2
4
8
Age (weeks)
b
+PFA
^{32}Pi uptake (cpm/mg)
6000
4000
600
400
200
0
2
4
8
Age (weeks)
c
^{3}H-glucose uptake (cpm/mg)
1500
1000
500
0
2
4
8
Age (weeks)

Figure 8

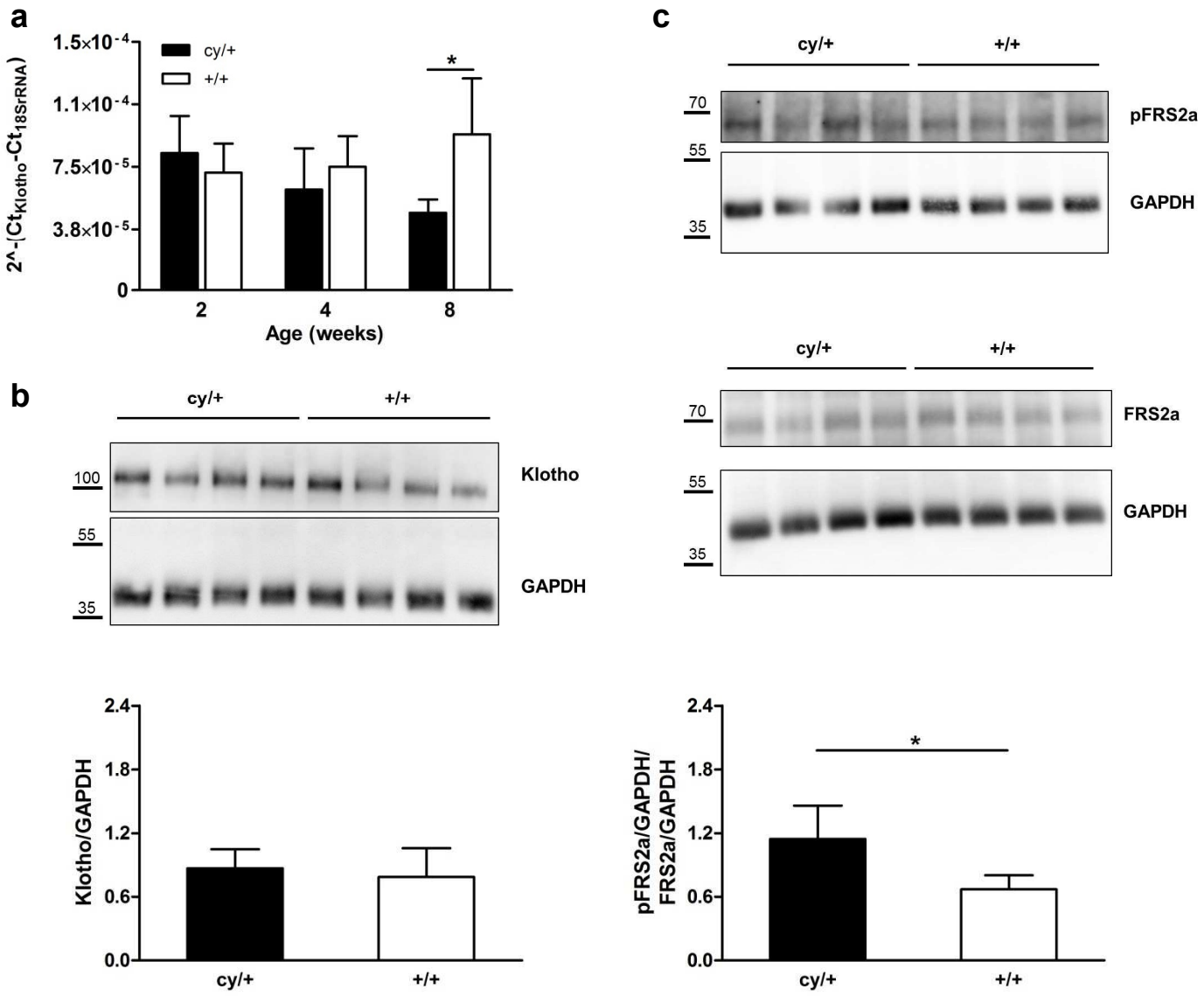
a
1.5×10-4
1.1×10-4
7.5×10-5
3.8×10-5
0
2^-(Ctklotho-Ct18SrRNA)
cy/+
+/+
*
2
4
8
Age (weeks)
b
cy/+
+/+
100
55
35
Klotho
GAPDH
Klotho/GAPDH
2.4
1.8
1.2
0.6
0.0
cy/+
+/+
c
cy/+
+/+
70
55
35
pFRS2a
GAPDH
cy/+
+/+
70
55
35
FRS2a
GAPDH
pFRS2a/GAPDH/
FRS2a/GAPDH
2.4
1.8
1.2
0.6
0.0
*
cy/+
+/+

Figure 9

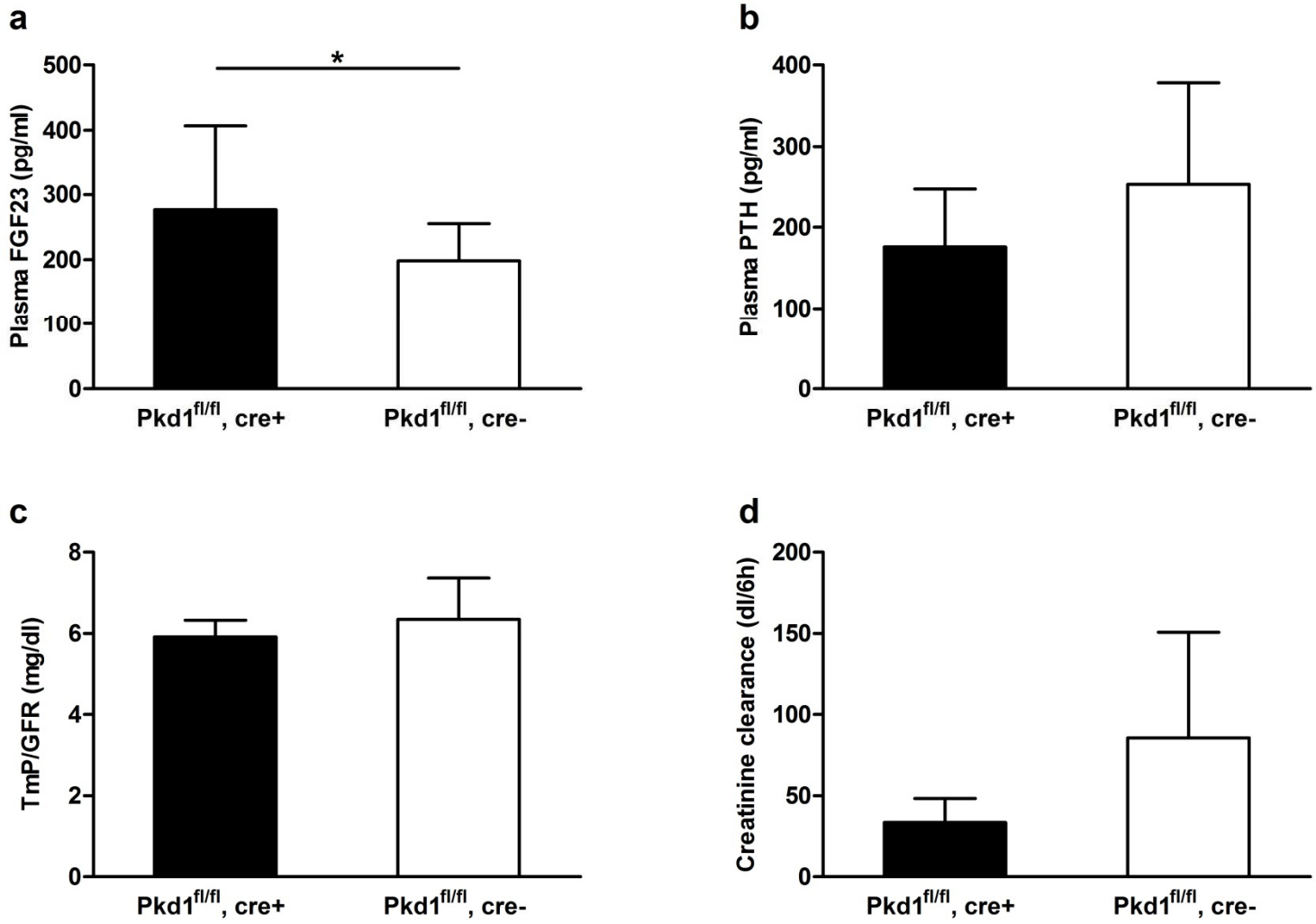
a
Plasma FGF23 (pg/ml)
500
400
300
200
100
0
*
Pkd1fl/fl, cre+
Pkd1fl/fl, cre-
b
Plasma PTH (pg/ml)
400
300
200
100
0
Pkd1fl/fl, cre+
Pkd1fl/fl, cre-
c
TmP/GFR (mg/dl)
8
6
4
2
0
Pkd1fl/fl, cre+
Pkd1fl/fl, cre-
d
Creatinine clearance (dl/6h)
200
150
100
50
0
Pkd1fl/fl, cre+
Pkd1fl/fl, cre-

Figure 10

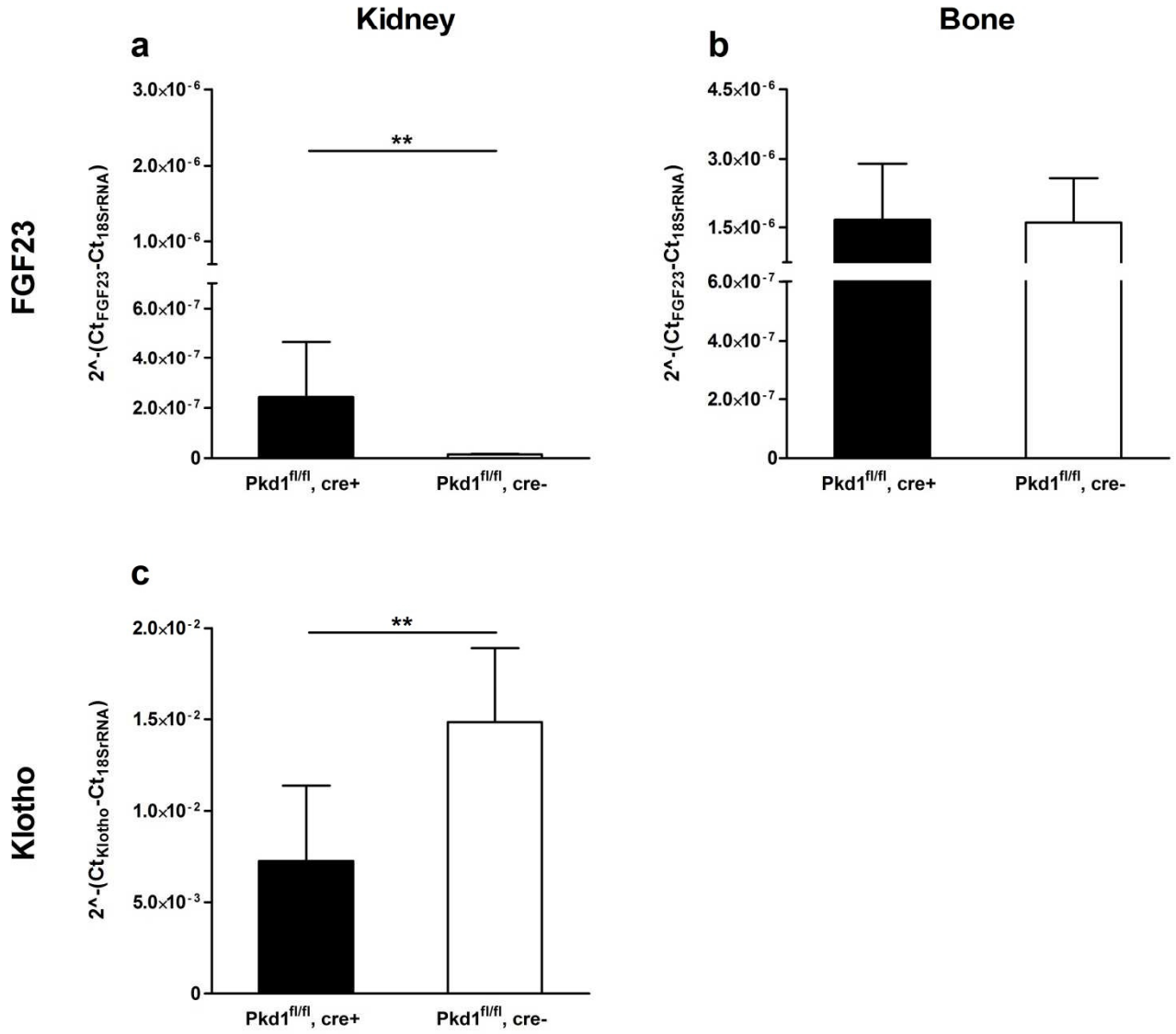
Kidney
Bone
a
b
c
FGF23
Klotho
2^-(Ct_FGF23-Ct_18SrRNA)
2^-(Ct_Klotho-Ct_18SrRNA)
3.0x10^-6
2.0x10^-6
1.0x10^-6
6.0x10^-7
4.0x10^-7
2.0x10^-7
0
4.5x10^-6
1.5x10^-6
2.0x10^-2
1.5x10^-2
1.0x10^-2
5.0x10^-3
**
Pkd1fl/fl, cre+
Pkd1fl/fl, cre-

SUPPLEMENTARY DATA TO:

Renal Expression of FGF23 and Peripheral Resistance to elevated FGF23 in Rodent Models of Polycystic Kidney Disease

Daniela Spichtig[1*], Hongbo Zhang[1*], Nilufar Mohebbi[1,2], Ivana Pavik[1], Katja Petzold[1], Gerti Stange[1], Lanja Saleh[3], Ilka Edenhofer[1], Stephan Segerer[1,2], Jürg Biber[1], Philippe Jaeger[4], Andreas L. Serra[1,2#], and Carsten A. Wagner[1#]

[1]Institute of Physiology and Zurich Center for Integrative Human Physiology (ZIHP), University of Zurich, Zurich Switzerland,

[2]Division of Nephrology, University Hospital Zurich, Switzerland,

[3]Department of Clinical Chemistry, University Hospital Zurich, Switzerland

[4]Center for Nephrology, Royal Free Hospital, University College London, UK

*D. Spichtig and H. Zhang contributed equally to this study and share first authorship

#A. L. Serra and C. A. Wagner contributed equally to this study and share last authorship

Please send correspondence to:

Carsten A. Wagner
Institute of Physiology
University of Zurich
Winterthurerstrasse 190
CH-8057 Zurich
Switzerland
Phone: +41-44-63 55023
Fax : +41-44-63 56814
Email: Wagnerca@access.uzh.ch

Supplementary Figures

Suppl. Figure 1

Renal function after fasting overnight of 4 weeks old HanSPRD rats. Plasma phosphate (a), plasma total calcium (b), TmP/GFR (c), and creatinine clearance after 4 weeks in cy/+ (black bars) and +/+ (white bars) HanSPRD rats; number of animals (median), cy/+ n = 12, +/+ n = 8

Suppl. Figure 2

mRNA expression of FGF23 regulatory molecules in kidney and bone. Relative mRNA expression of Fam20c and Dmp1 in kidney (a, c) and bone (b, d) after 4 and 8 weeks in cy/+ (black bars) and +/+ (white bars) Han:SPRD rats; number of animals (median), cy/+ n = 7, +/+ n = 5; * $p<0.05$

Suppl. Figure 3

Immunolocalization of NaPi-IIa. Frozen kidney sections were stained with antibodies against NaPi-IIa (red), Phalloidin-FITC for actin (green), and DAPI (blue) in cy/+ and +/+ animals after 4 and 8 weeks. Scale bar 50 µm.

Suppl. Figure 4

Heart wall thickness and heart weight. Heart wall (a) and septum thickness (c) of 4 weeks old HanSPRD rats; heart weight of 10 weeks old rats normalized to body weight (b) and tibia length (d); number of animals (median), cy/+ = 5, +/+ = 4

Suppl. Figure 5

FGFR-1 mRNA expression. Relative mRNA expression of the FGF receptor 1 (FGFR-1) in bone (a) and kidney (b) to 18S rRNA after 2, 4, and 8 weeks in cy/+ (black bars) and +/+ (white bars) Han:SPRD rats (mean ±SD); number of animals (median), cy/+ n = 6, +/+ n = 5

Suppl. Figure 6

Pkd1 mRNA expression. Relative Pkd1 mRNA abundance in kidney (a) and bone (b) of 10 weeks old *Pkd1*$^{fl/fl}$, cre+ (black bars) compared to *Pkd1*$^{fl/fl}$, cre- (white bars)

mice (mean ±SD); number of animals (median), $Pkd1^{fl/fl}$, cre+ n = 8, $Pkd1^{fl/fl}$, cre- n = 15; ** p<0.001

Suppl. Figure 7

Expression of FGF23 in kidneys from *Pkd*$^{fl/fl}$, cre+ KO mice. Frozen kidney sections were stained for FGF23 (green), calbindin D28k, a marker of DCT and CNT segments (red), and DAPI (cell nuclei). In kidneys from *Pkd1*$^{fl/fl}$, cre+ mice strong FGF23 staining is observed in cells lining the cysts (a,b), no staining for FGF23 is observed in kidneys from *Pkd1*$^{fl/fl}$, cre- mice (c,d). Omission of primary antibodies in P *Pkd1*$^{fl/fl}$, cre+ kidneys showed no staining (e). Original magnification 400 x.

Supplementary Table 1

Primer and probe sequences used for RT-PCR

Gene	Primers	Probe
Rat NaPi-IIa (Slc34a1)	F: 5'-GGAATCACAGTDTCATTCGGATT-3'	5'-TGTCAACCAGAGACAAAAGA GGCTTCCACT-3'
	R: 5'-ATGGCCTCTACCCTGGACATAG-3'	
Rat NaPi-IIc (Slc34a3)	F: 5'-GGGATCGGGATGAATTTCAGA-3'	5'-ACGGCATCTTCAACTGGCTC ACAGTGTT-3'
	R: 5'-GGGCCAGCTCACTCAGTCTCT-3'	
Rat FGF23	F: 5'-GCAACATTTTTGGATCGTATCA-3'	5'-AGATTCCGCCAGTGGACGCT AGAGA-3'
	R: 5'-GATGCTTCGGTGACAGGTAGA-3'	
Rat Klotho	F: 5'-TATCTCAAGAAGTTCATAATGGAAAGC-3'	5'-TAAAAGCCATCAGGCTGGAT GGGG-3'
	R: 5'-GAGGGACCATGCGGTGTA-3'	
Rat FGFR1	F: 5'-GGTTGAAAAATGGCAAGGAA-3'	5'-TCGGAGGCTACAAGGTTCGT TACGC-3'
	R: 5'-CCACGATGCAGGTGTAGTTG-3'	
Rat Cyp24a1	F: 5'-CAAATCAGTCAAACCCTGCAT-3'	5'-TACAGAGATATTCCCAGCAG CCCGG-3'
	R: 5'-GGCGTACAGTTCCTTCTTGG-3'	
Rat Cyp27b1	F: 5'-TGGCAAACGAAGTTGCATAG-3'	5'-CTACAAATGGCGTTGGCCCA GATC-3'
	R: 5'-AGCACCTCAAAATGGGTCAA-3'	
Rat Fam20c	F: 5'-CCATCGATGCCTTACTCCAC-3'	5'-CAGAAGATCACCAGTGTCGC CATGA-3'
	R: 5'-CCCGTAATTCTGGAAGGTCA-3'	
Rat Dmp1	F: 5'-CTGTCCTGTGCTCTCCCTGT-3'	5'-TCTGAAAGCTCCGAAGAGAG

	R: 5'-GCTGTCCGTGTGGTCACTATT-3'	GACGG-3'
Mouse Pkd1	F: 5'-GGCCAACCTCTCCTCAGTATC-3'	5’-CTGTGGTGAGGAATATGTCG
	R: 5'-GAAGGGTACTGCTGCCACA-3'	CCTGC-3’
Mouse FGF23	F: 5'-TCGAAGGTTCCTTTGTATGGAT-3'	5'-TTTTTGGATCGCTTCACT-3'
	R: 5'-AGTGATGCTTCTGCGACAAGT-3'	
Mouse Klotho	F: 5'-ACGTTCAAGTGGACACTACTCTCTC-3'	5'-CCGAATGTCTATCTGTGGGA
	R: 5'-TTGGCTACAACCCCGTCTAC-3'	TGTGCA-3'

Supplementary Methods

H&E histology

Hearts were fixed in 10% buffered formalin over night and embedded in paraffin. Sections were stained with Hematoxilin-Eosin following routine protocols.

Supplementary Figure 1

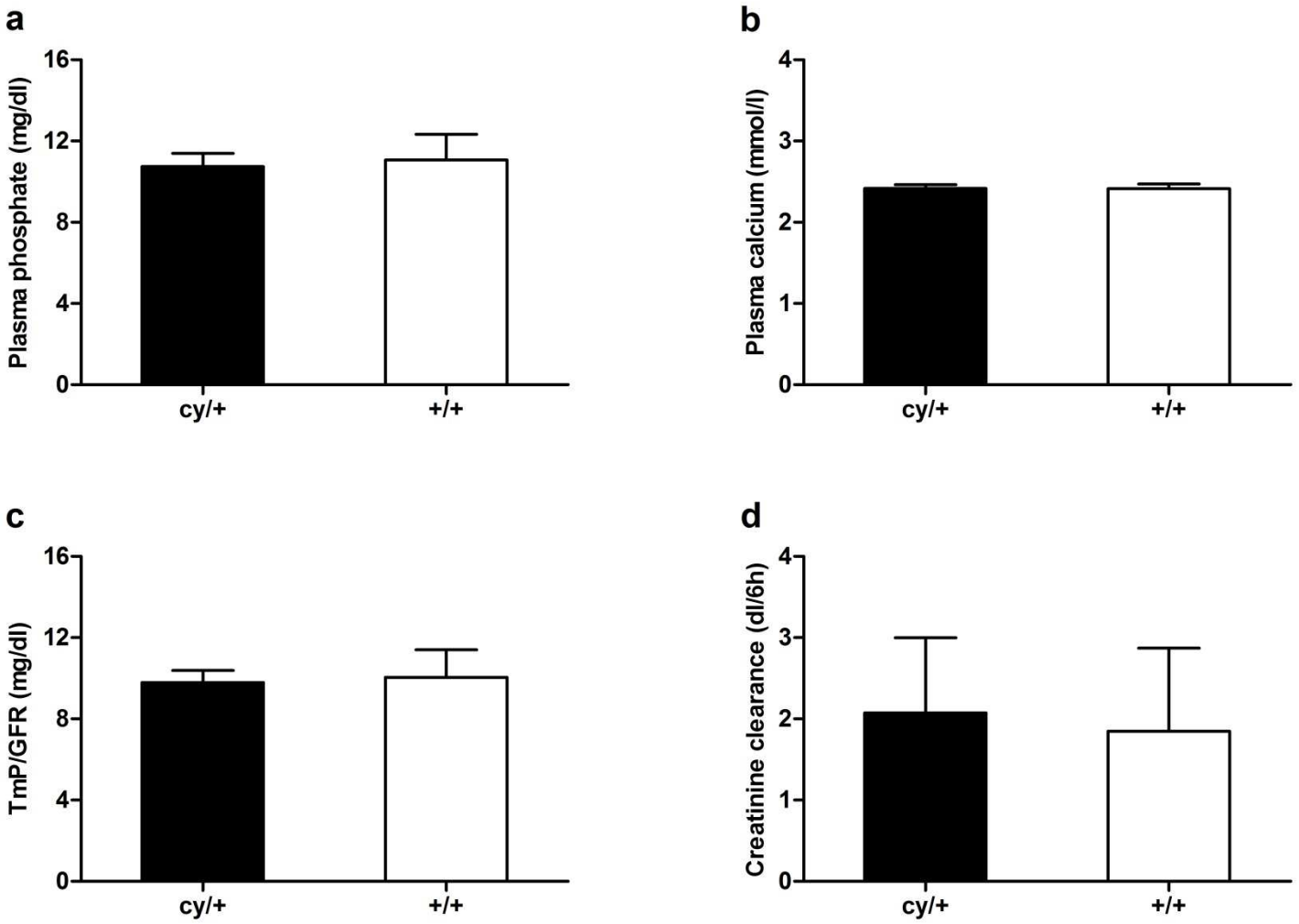

Supplementary Figure 2

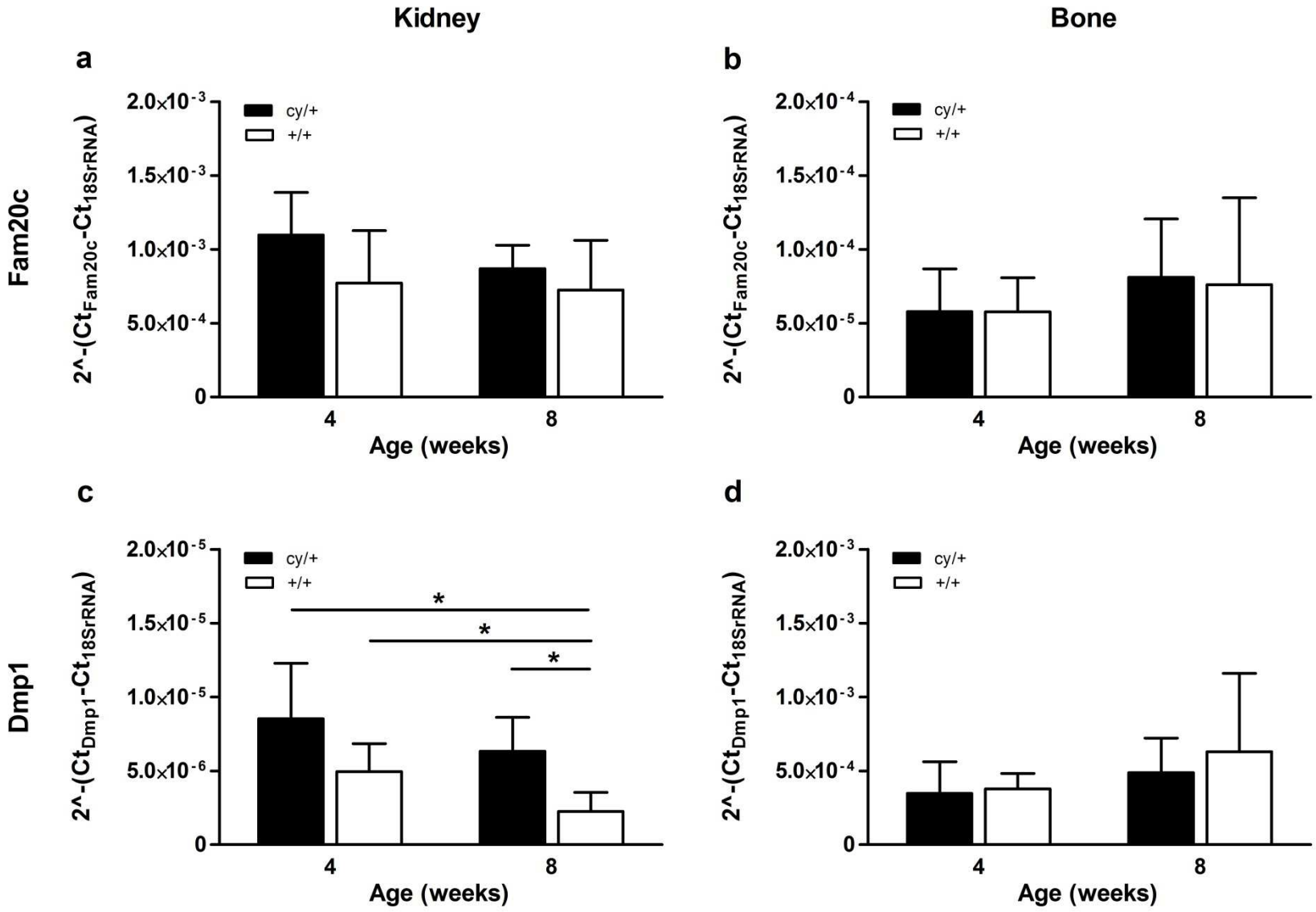

Supplementary Figure 3

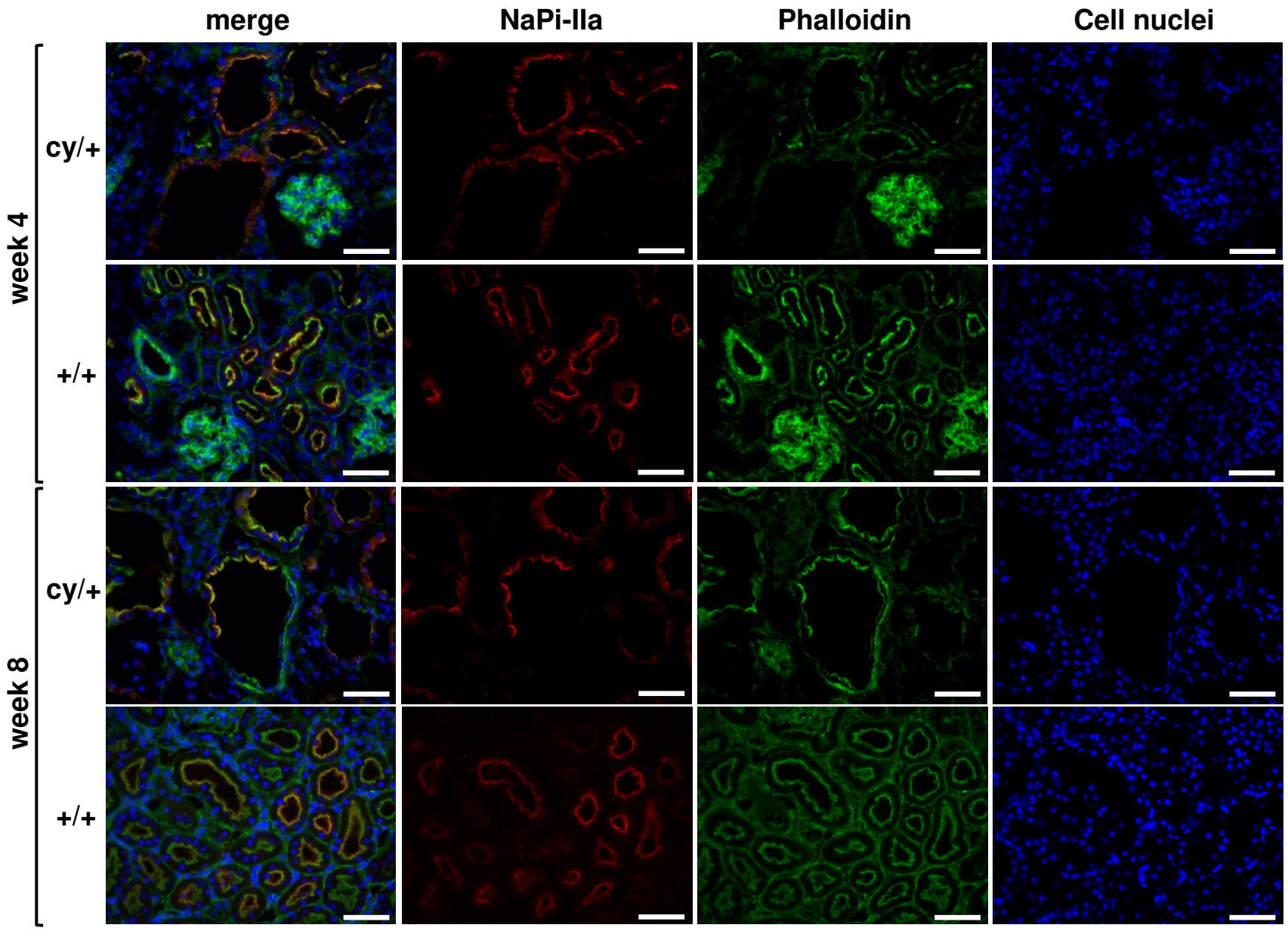

Supplementary Figure 4

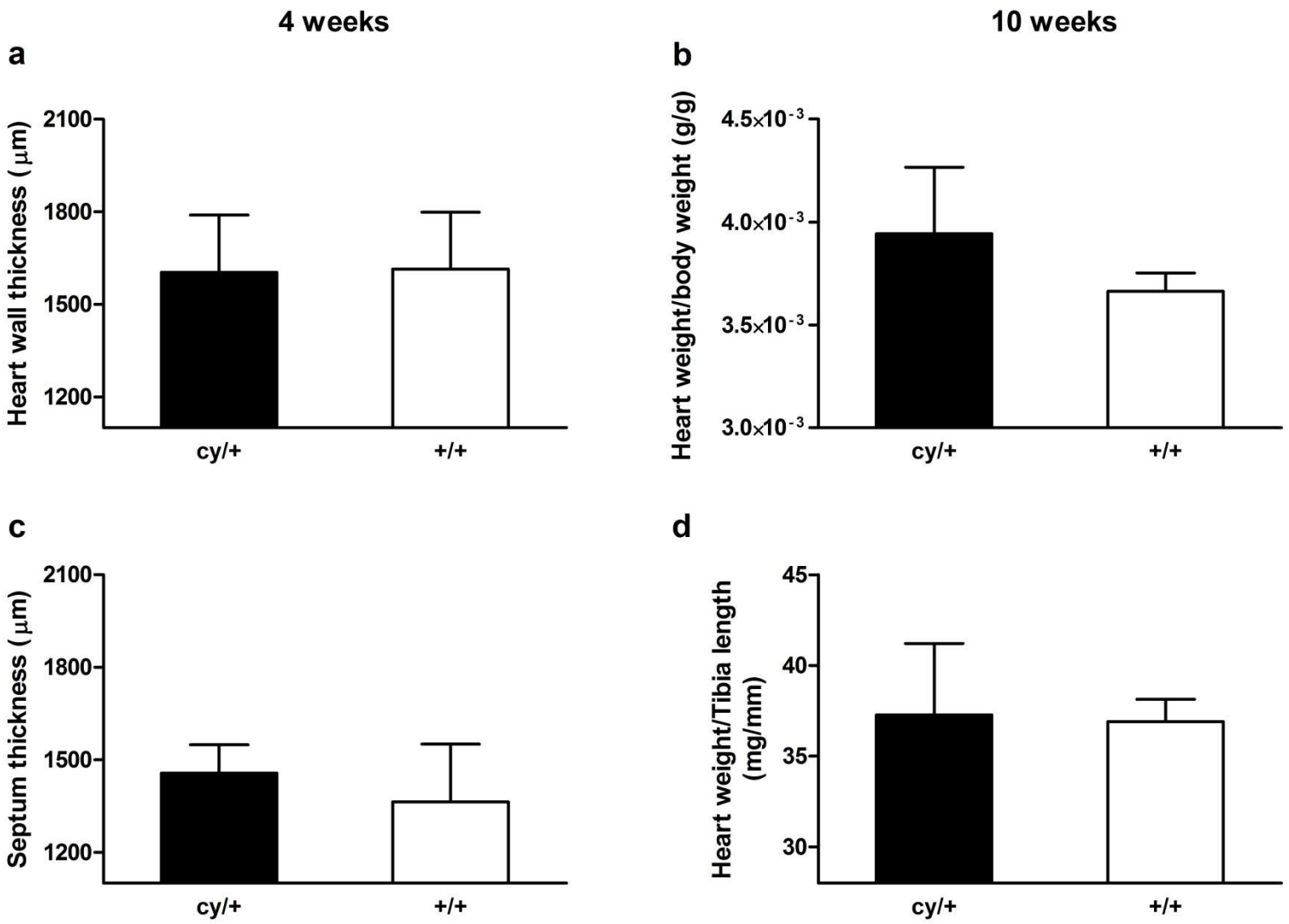

Supplementary Figure 5

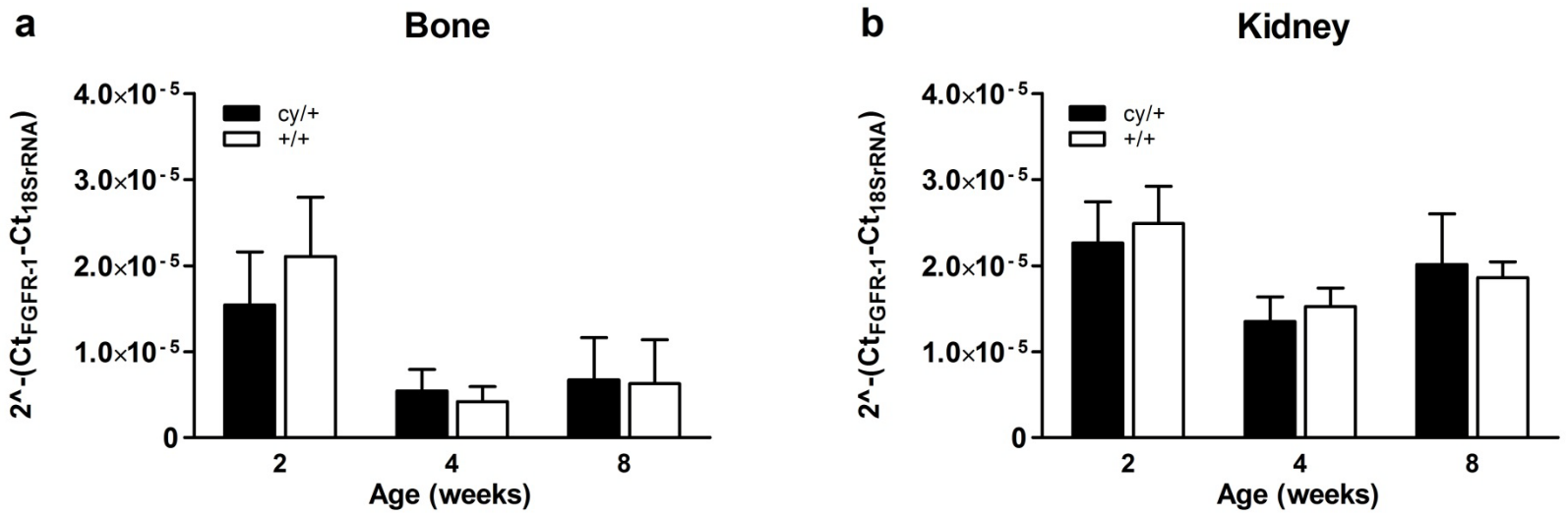

Supplementary Figure 6

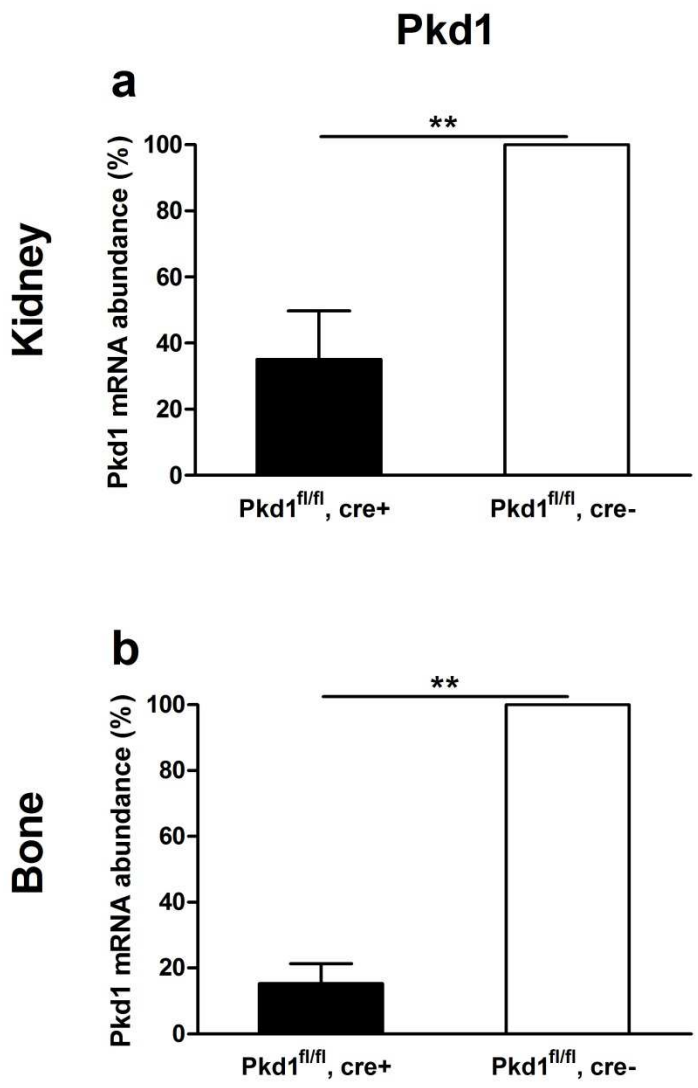

Supplementary Figure 7